3 Magnetism: Models and Mechanisms

Eva Pavarini
Institute for Advanced Simulation
Forschungszentrum Jülich

Contents

E. Pavarini, E. Koch, and U. Schollwöck
Emergent Phenomena in Correlated Matter
Modeling and Simulation Vol. 3
Forschungszentrum Jülich, 2013, ISBN 978-3-89336-884-6
http://www.cond-mat.de/events/correl13

1 Magnetism in strongly-correlated systems

Long-range magnetic order is a manifestation of emergence, the hallmark of strong electron-electron correlations. It arises from the same interactions that lead to the metal-insulator transition and orbital-ordering or that give rise to the Kondo effect. And yet, magnetic order phenomena can, to a large extent, be explained by solving spin models and forgetting about the microscopic mechanisms which justify them. To understand models and mechanisms we have, however, to take a step back into the complex world of strong correlations [1–7].

Magnetism ultimately arises from the intrinsic magnetic moment of electrons, $\boldsymbol{\mu} = -g\mu_B \boldsymbol{s}$, where μ_B is the Bohr magneton and $g \simeq 2.0023$ is the electronic g-factor. It is however an inherently quantum mechanical effect, the consequence of the interplay between Pauli exclusion principle, Coulomb electron-electron interaction, and hopping of electrons. To understand this let us consider the simplest possible system, an isolated atom or ion. In the non-relativistic limit electrons in a single ion are typically described by the Hamiltonian

$$H_e^{\rm NR} = -\frac{1}{2}\sum_i \nabla_i^2 - \sum_i \frac{Z}{r_i} + \sum_{i>j} \frac{1}{|\boldsymbol{r}_i - \boldsymbol{r}_j|},$$

where Z is the atomic number and $\{\boldsymbol{r}_i\}$ are the coordinates of the electrons with respect to the ionic nucleus. Here, as in the rest of this lecture, we use atomic units. If we consider only the external atomic shell with quantum numbers nl, for example the $3d$ shell of transition-metal ions, we can rewrite this Hamiltonian as follows

$$H_e^{\rm NR} = \varepsilon_{nl} \sum_{m\sigma} c^\dagger_{m\sigma} c_{m\sigma} + \frac{1}{2}\sum_{\sigma\sigma'} \sum_{m\tilde{m}m'\tilde{m}'} U^l_{mm'\tilde{m}\tilde{m}'} c^\dagger_{m\sigma} c^\dagger_{m'\sigma'} c_{\tilde{m}'\sigma'} c_{\tilde{m}\sigma}. \qquad (1)$$

Here ε_{nl} is the energy of the electrons in the nl atomic shell and m the degenerate one-electron states in that shell. For a hydrogen-like atom

$$\varepsilon_{nl} = -\frac{1}{2}\frac{Z^2}{n^2}.$$

The couplings $U^l_{mm'\tilde{m}\tilde{m}'}$ are the four-index Coulomb integrals. In a basis of atomic functions the bare Coulomb integrals are

$$U^{iji'j'}_{mm'\tilde{m}\tilde{m}'} = \int d\boldsymbol{r}_1 \int d\boldsymbol{r}_2 \, \frac{\overline{\psi_{im\sigma}}(\boldsymbol{r}_1)\overline{\psi_{jm'\sigma'}}(\boldsymbol{r}_2)\psi_{j'\tilde{m}'\sigma'}(\boldsymbol{r}_2)\psi_{i'\tilde{m}\sigma}(\boldsymbol{r}_1)}{|\boldsymbol{r}_1 - \boldsymbol{r}_2|},$$

and

$$U^l_{mm'\tilde{m}\tilde{m}'} = U^{iiii}_{mm'\tilde{m}\tilde{m}'} \qquad m, m', \tilde{m}, \tilde{m}' \in nl \text{ shell}.$$

The eigenstates of Hamiltonian (1) for fixed number of electrons, N, are the multiplets [8, 9]. Since in $H_e^{\rm NR}$ the Coulomb repulsion and the central potential are the only interactions, the multiplets can be labeled with S and L, the quantum numbers of the electronic total spin and total orbital angular momentum operators, $\boldsymbol{S} = \sum_i \boldsymbol{s}_i$, and $\boldsymbol{L} = \sum_i \boldsymbol{l}_i$. Closed-shell ions have $S = L = 0$ in their ground state. Ions with a partially-filled shell are called *magnetic ions*; the value of S and L for their ground state can be obtained via two rules due to Friedrich Hund. They say that the lowest-energy multiplet is the one with

- the largest value of S
- the largest value of L compatible with the previous rule

The main relativistic effect is the spin-orbit interaction, which has the form $H_e^{\rm SO} = \sum_i \lambda_i \, \boldsymbol{l}_i \cdot \boldsymbol{s}_i$. For not too heavy atoms it is a weak perturbation. Then, for electrons in a given shell, we can use the first and second Hund's rule to rewrite $H_e^{\rm SO}$ in a simpler form

$$\begin{aligned} H_e^{\rm SO} &\sim \lambda \, \boldsymbol{L} \cdot \boldsymbol{S} = \frac{1}{2} \, \lambda \, \left(\boldsymbol{J}^2 - \boldsymbol{S}^2 - \boldsymbol{L}^2 \right) , \\ \lambda &\sim \left[2\Theta(1-2n) - 1 \right] \, g\mu_B^2 \, \frac{1}{2S} \left\langle \frac{1}{r} \frac{d}{dr} v_{\rm R}(r) \right\rangle , \end{aligned} \tag{2}$$

where n is the filling and Θ the step function; $v_{\rm R}(r)$ is the effective potential, which includes, e.g., the Hartree electron-electron term [10]. For a hydrogen-like atom, $v_{\rm R}(r) = -Z/r$. Because of the LS coupling (2) the eigenstates have quantum numbers L, S and J, where $\boldsymbol{J} = \boldsymbol{S} + \boldsymbol{L}$ is the total angular momentum. The value of J in the ground-state multiplet is given by the third Hund's rule

- total angular momentum $J = \begin{cases} |L-S| & \text{for filling } n < 1/2 \\ S & \text{for filling } n = 1/2 \\ L+S & \text{for filling } n > 1/2 \end{cases}$

In the presence of spin-orbit interaction a given multiplet is then labeled by ${}^{2S+1}L_J$, and its states can be indicated as $|JJ_zLS\rangle$. If we consider, e.g., the case of the ion Cu^{2+}, characterized by the [Ar] $3d^9$ electronic configuration, Hund's rules tell us that the $3d$ ground-state multiplet has quantum numbers $S = 1/2$, $L = 2$ and $J = 5/2$. A Mn^{3+} ion, which is in the [Ar] $3d^4$ electronic configuration, has instead a ground-state multiplet with quantum numbers $S = 2$, $L = 2$ and $J = 0$. The order of the Hund's rules reflects the hierarchy of the interactions. The strongest interactions are the potential $v_{\rm R}(r)$, which determines ε_{nl}, and the average Coulomb interaction, the strength of which is measured by the average *direct Coulomb integral*,

$$U_{\rm avg} = \frac{1}{(2l+1)^2} \sum_{mm'} U^l_{mm'mm'} .$$

For a N-electron state the energy associated with these two interactions is $E(N) = \varepsilon_{nl} N + U_{\rm avg} N(N-1)/2$, the same for all multiplets of a given shell. The first Hund's rule is instead due to the average *exchange Coulomb integral*, $J_{\rm avg}$, defined as

$$U_{\rm avg} - J_{\rm avg} = \frac{1}{2l(2l+1)} \sum_{mm'} \left(U^l_{mm'mm'} - U^l_{mm'm'm} \right) ,$$

which is the second largest Coulomb term; for transition-metal ions $J_{\rm avg} \sim 1$ eV. Smaller Coulomb integrals determine the orbital anisotropy of the Coulomb matrix and the second Hund's rule.[1] The third Hund's rule comes, as we have seen, from the spin-orbit interaction which, for not too heavy atoms, is significantly weaker than all the rest.

[1] For more details on Coulomb integrals and their averages see Ref. [10].

The role of Coulomb electron-electron interaction in determining S and L can be understood through the simple example of a C atom, electronic configuration [He] $2s^2\ 2p^2$. We consider only the p shell, filled by two electrons. The Coulomb exchange integrals have the form

$$\begin{aligned} J^p_{m,m'} &= U^p_{mm'm'm} \\ &= \int d\boldsymbol{r}_1 \int d\boldsymbol{r}_2 \, \frac{\overline{\psi_{im\sigma}}(\boldsymbol{r}_1)\overline{\psi_{im'\sigma}}(\boldsymbol{r}_2)\psi_{im\sigma}(\boldsymbol{r}_2)\psi_{im'\sigma}(\boldsymbol{r}_1)}{|\boldsymbol{r}_1-\boldsymbol{r}_2|} \\ &= \int d\boldsymbol{r}_1 \int d\boldsymbol{r}_2 \, \frac{\phi_{imm'\sigma}(\boldsymbol{r}_1)\overline{\phi_{imm'\sigma}}(\boldsymbol{r}_2)}{|\boldsymbol{r}_1-\boldsymbol{r}_2|} = \frac{1}{V}\sum_{\boldsymbol{k}} \frac{4\pi}{k^2}\left|\phi_{imm'\sigma}(\boldsymbol{k})\right|^2, \end{aligned} \tag{3}$$

and they are therefore positive. They generate the Coulomb-interaction term

$$-\frac{1}{2}\sum_{\sigma}\sum_{m\neq m'} J^p_{m,m'} c^\dagger_{m\sigma}c_{m\sigma}c^\dagger_{m'\sigma}c_{m'\sigma} = -\frac{1}{2}\sum_{m\neq m'} 2J^p_{m,m'}\left[S^m_z S^{m'}_z + \frac{1}{4}n_m n'_m\right].$$

This interaction yields an *energy gain* if the two electrons occupy two different p orbitals with parallel spins, hence favors the state with the largest spin (first Hund's rule). It turns out that for the p^2 configuration there is only one possible multiplet with $S=1$, and such a state has $L=1$. There are instead two excited $S=0$ multiplets, one with $L=0$ and the other with $L=2$; the latter is the one with the lowest energy (second Hund's rule).

To understand the magnetic properties of an isolated ion we have to analyze how its levels are modified by an external magnetic field $\boldsymbol{h}$. The effect of a magnetic field is described by

$$H^{\rm H}_e = \mu_B\left(g\boldsymbol{S}+\boldsymbol{L}\right)\cdot\boldsymbol{h} + \frac{h^2}{8}\sum_i\left(x_i^2+y_i^2\right) = H^{\rm Z}_e + H^L_e. \tag{4}$$

The linear term is the Zeeman Hamiltonian. If the ground-state multiplet is characterized by $J\neq 0$ the Zeeman interaction splits its $2J+1$ degenerate levels. The second order term yields Larmor diamagnetism, which is usually only important if the ground-state multiplet has $J=0$, as it happens for ions with closed external shells. The energy $\mu_B h$ is typically very small (for a field as large as 100 T it is as small as 6 meV); it can however be comparable with or larger than the spin-orbit interaction if the latter is tiny (very light atoms). Taking all interactions into account, the total Hamiltonian is

$$H_e \sim H^{\rm NR}_e + H^{\rm SO}_e + H^{\rm H}_e.$$

In a crystal the electronic Hamiltonian is complicated by the interaction with other nuclei and their electrons. The non-relativistic part of the Hamiltonian takes then the form

$$H^{\rm NR}_e = -\frac{1}{2}\sum_i \nabla^2_i + \frac{1}{2}\sum_{i\neq i'}\frac{1}{|\boldsymbol{r}_i-\boldsymbol{r}_{i'}|} - \sum_{i\alpha}\frac{Z_\alpha}{|\boldsymbol{r}_i-\boldsymbol{R}_\alpha|} + \frac{1}{2}\sum_{\alpha\neq\alpha'}\frac{Z_\alpha Z_{\alpha'}}{|\boldsymbol{R}_\alpha-\boldsymbol{R}_{\alpha'}|},$$

where Z_α is the atomic number of the nucleus located at position $\boldsymbol{R}_\alpha$. In a basis of localized Wannier functions [10] this Hamiltonian can be written as

$$\begin{aligned} H^{\rm NR}_e &= -\sum_{ii'\sigma}\sum_{mm'} t^{i,i'}_{m,m'} c^\dagger_{im\sigma}c_{i'm'\sigma} \\ &\quad + \frac{1}{2}\sum_{ii'jj'}\sum_{\sigma\sigma'}\sum_{mm'}\sum_{\tilde{m}\tilde{m}'} U^{iji'j'}_{mm'\tilde{m}\tilde{m}'} c^\dagger_{im\sigma}c^\dagger_{jm'\sigma'}c_{j'\tilde{m}'\sigma'}c_{i'\tilde{m}\sigma}, \end{aligned} \tag{5}$$

where

$$t^{i,i'}_{m,m'} = -\int d\boldsymbol{r}\, \overline{\psi_{im\sigma}}(\boldsymbol{r}) \left[-\frac{1}{2}\nabla^2 + v_{\rm R}(\boldsymbol{r})\right] \psi_{i'm'\sigma}(\boldsymbol{r}).$$

The terms $\varepsilon_{m,m'} = -t^{i,i}_{m,m'}$ yield the crystal-field matrix and $t^{i,i'}_{m,m'}$ with $i \neq i'$ the hopping integrals. The label m indicates here the orbital quantum number of the Wannier function. In general the Hamiltonian (5) will include states stemming from more than a single atomic shell. For example, in the case of strongly-correlated transition-metal oxides, the set $\{im\}$ includes transition-metal $3d$ and oxygen $2p$ states. The exact solution of the many-body problem described by (5) is an impossible challenge. The reason is that the properties of a many-body system are inherently emergent and hence hard to predict *ab-initio* in the lack of any understanding of the mechanism behind them. In this lecture, however, we want to focus on magnetism. Since the nature of cooperative magnetic phenomena in crystals is nowadays to a large extent understood, we can find realistic approximations to (5) and even map it onto simpler models which still retain the essential ingredients to explain long-range magnetic order.

Let us identify the parameters of the electronic Hamiltonian important for magnetism. The first is the crystal-field matrix $\varepsilon_{m,m'}$. The crystal field at a given site i is a non-spherical potential due to the joint effect of the electric field generated by the surrounding ions and of covalent-bond formation [9]. The crystal field might split the levels within a given shell and has therefore a strong impact on magnetic properties. We can identify three ideal regimes. In the *strong crystal field* limit the crystal field splitting is so large that it is comparable with the average Coulomb exchange responsible for the first Hund's rule. This can happen in $4d$ or $5d$ transition-metal oxides. A consequence of an *intermediate crystal field* (weaker than the average Coulomb exchange but larger than Coulomb anisotropy and spin-orbit interaction) is the quenching of the angular momentum, $\langle \boldsymbol{L} \rangle = 0$. In this limit the second and third Hund's rule are not respected. This typically happens in $3d$ transition-metal oxides. In $4f$ systems the crystal-field splitting is usually much weaker than the spin-orbit coupling (*weak crystal field* limit) and mainly splits states within a given multiplet, leaving a reduced magnetic moment. In all three cases, because of the crystal field, a magnetic ion in a crystal might lose, totally or partially, its spin, angular or total moment. Or, sometimes, it is the other way around. This happens for Mn^{3+} ions, which should have a $J = 0$ ground state according to the third Hund's rule. However in perovskites such as $LaMnO_3$ they behave as $S = 2$ ions because of the quenching of the angular momentum. Even if the crystal field does not suppress the magnetic moment of the ion, the electrons might delocalize to form broad bands completely losing their original atomic character. This happens, e.g., if the hopping integrals $t^{i,i'}_{m,m'}$ are much larger than the average on-site Coulomb interaction $U_{\rm avg}$. Surprisingly, magnetic instabilities arise even in the absence of localized moments. This *itinerant magnetism* is mostly due to band effects, i.e., it is associated with a large one-electron linear static response-function, $\chi_0(\boldsymbol{q}; 0)$. In this limit correlation effects are typically weak. To study them we can exploit the power of the *standard model* of solid-state physics, the density-functional theory (DFT), taking into account Coulomb interaction effects beyond the local-density approximation (LDA) at the perturbative level, e.g., in the random-phase approximation (RPA). With this approach we can understand and describe Stoner instabilities.

In the opposite limit, the *local moments* regime, the hopping integrals are small with respect to $U_{\rm avg}$. This is the regime of strong electron-electron correlations, where complex many-body effects, e.g., those leading to the Mott metal-insulator transition, play an important role. At *low enough energy*, however, only spin excitations matter. Ultimately, at integer filling we can integrate out (*downfold*) charge fluctuations and describe the system via effective spin Hamiltonians. The latter typically take the form

$$H_{\rm S} \;=\; \frac{1}{2}\sum_{ii'} \Gamma^{i,i'}\; \boldsymbol{S}_i \cdot \boldsymbol{S}_{i'} + \cdots = H_{\rm S}^H + \ldots . \tag{6}$$

The term $H_{\rm S}^H$ given explicitly in (6) is the Heisenberg Hamiltonian, and $\Gamma^{i,i'}$ is the Heisenberg exchange coupling, which can be antiferromangetic ($\Gamma^{i,i'} > 0$) or ferromagnetic ($\Gamma^{i,i'} < 0$). The Hamiltonian (6) can, for a specific system, be quite complicated, and might include long-range exchange interactions or anisotropic terms. Nevertheless, it represents a huge simplification compared to the unsolvable many-body problem described by (5), since, at least within very good approximated schemes, it can be solved. Spin Hamiltonians of type (6) are the minimal models which still provide a realistic picture of long-range magnetic order in strongly-correlated insulators. There are various sources of exchange couplings. Electron-electron repulsion itself yields via Coulomb exchange a ferromagnetic Heisenberg interaction, the *Coulomb exchange interaction*. The origin of such interaction can be understood via a simple model with a single orbital, m. The inter-site Coulomb exchange coupling has then the form

$$J^{i,i'} = U^{ii'i'i}_{mmmm} \;=\; \int d\boldsymbol{r}_1 \int d\boldsymbol{r}_2 \; \frac{\overline{\psi_{im\sigma}}(\boldsymbol{r}_1)\overline{\psi_{i'm\sigma}}(\boldsymbol{r}_2)\psi_{im\sigma}(\boldsymbol{r}_2)\psi_{i'm\sigma}(\boldsymbol{r}_1)}{|\boldsymbol{r}_1 - \boldsymbol{r}_2|},$$

and it is therefore positive, as one can show by following the same steps that we used in Eq. (3) for $J^p_{m,m'}$. Hence, the corresponding Coulomb interaction yields a ferromagnetic Heisenberg-like Hamiltonian with $\Gamma^{i,i'} = -2J^{i,i'} < 0$. A different source of magnetic interactions are the *kinetic exchange* mechanisms (direct exchange, super-exchange, double exchange, Rudermann-Kittel-Kasuya-Yosida interaction ...), which are mediated by the hopping integrals. Kinetic exchange couplings are typically (with few well understood exceptions) antiferromagnetic [11]. A representative example of kinetic exchange will be discussed in the next section.

While itinerant and local moment regime are very interesting ideal limit cases, correlated materials elude rigid classifications. The same system can present features associated with both regimes, although at different temperatures and/or energy scales. This happens in Kondo systems, heavy Fermions, metallic strongly-correlated materials, and doped Mott insulators.

In this lecture we will discuss in representative cases the itinerant and localized moment regime and their crossover, as well as the most common mechanisms leading to magnetic cooperative phenomena. Since our target is to understand strongly-correlated materials, we adopt the formalism typically used for these systems. A concise introduction to Matsubara Green functions, correlation functions, susceptibilities and linear-response theory can be found in the Appendix.

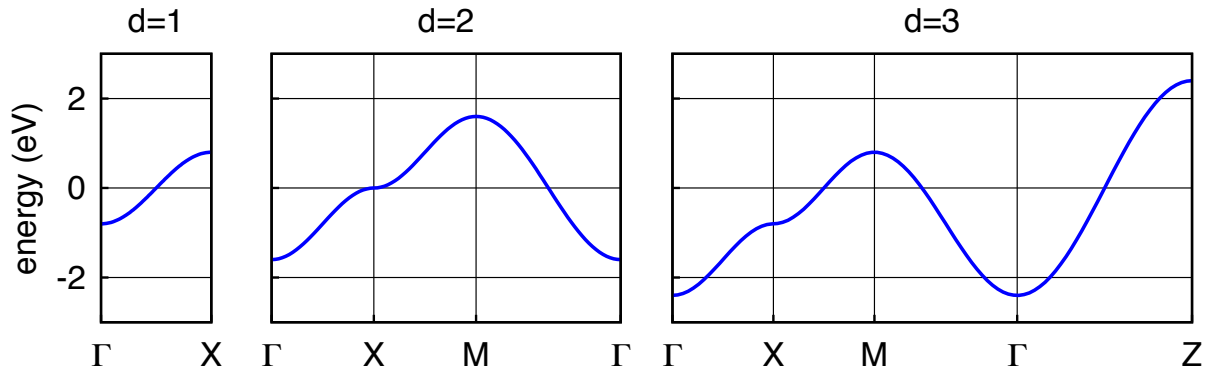

Fig. 1: *The band structure of the one-band tight-binding model (hypercubic lattice). The hopping integral is $t = 0.4$ eV. From left to right: one-, two-, and three-dimensional case. At half-filling ($n = 1$) the Fermi level is at zero energy.*

2 The Hubbard model

The simplest model that we can consider is the one-band Hubbard model

$$H = \varepsilon_d \sum_i \sum_\sigma c^\dagger_{i\sigma} c_{i\sigma} - t \sum_{\langle ii' \rangle} \sum_\sigma c^\dagger_{i\sigma} c_{i'\sigma} + U \sum_i n_{i\uparrow} n_{i\downarrow} = H_d + H_T + H_U, \tag{7}$$

where ε_d is the on-site energy, t is the hopping integral between first nearest neighbors $\langle ii' \rangle$ and U the on-site Coulomb repulsion; $c^\dagger_{i\sigma}$ creates an electron in a Wannier state with spin σ centered at site i and $n_{i\sigma} = c^\dagger_{i\sigma} c_{i\sigma}$. The Hubbard model is a simplified version of Hamiltonian (5) with $m = m' = \tilde{m} = \tilde{m}' = 1$ and

$$\begin{cases} \varepsilon_d &= -t^{i,i}_{1,1} \\ t &= t^{\langle i,i' \rangle}_{1,1} \\ U &= U^{iiii}_{1111} \end{cases} .$$

In the $U = 0$ limit the Hubbard model describes a system of independent electrons. The Hamiltonian is then diagonal in the Bloch basis

$$H_d + H_T = \sum_{\boldsymbol{k}} \sum_\sigma [\varepsilon_d + \varepsilon_{\boldsymbol{k}}] c^\dagger_{\boldsymbol{k}\sigma} c_{\boldsymbol{k}\sigma}. \tag{8}$$

The energy dispersion $\varepsilon_{\boldsymbol{k}}$ depends on the geometry and dimensionality d of the lattice. For a hypercubic lattice in d dimensions

$$\varepsilon_{\boldsymbol{k}} = -2t \sum_{\nu=1}^{d} \cos(k_{r_\nu} a),$$

where a is the lattice constant, and $r_1 = x, r_2 = y, r_3 = z$. The energy $\varepsilon_{\boldsymbol{k}}$ does not depend on the spin. In Fig. 1 we show $\varepsilon_{\boldsymbol{k}}$ in the one-, two- and three-dimensional case.

In the opposite limit ($t = 0$) the Hubbard model describes a collection of isolated atoms. Each atom has four electronic many-body states

$$\begin{array}{lcll|lll} |N,S,S_z\rangle & & & & N & S & E(N) \\ \hline |0,0,0\rangle & = & |0\rangle & & 0 & 0 & 0 \\ |1,\tfrac{1}{2},\uparrow\rangle & = & c^\dagger_{i\uparrow}|0\rangle & & 1 & 1/2 & \varepsilon_d \\ |1,\tfrac{1}{2},\downarrow\rangle & = & c^\dagger_{i\downarrow}|0\rangle & & 1 & 1/2 & \varepsilon_d \\ |2,0,0\rangle & = & c^\dagger_{i\uparrow}c^\dagger_{i\downarrow}|0\rangle & & 2 & 0 & 2\varepsilon_d + U \end{array} \tag{9}$$

where $E(N)$ is the total energy, N the total number of electrons and S the total spin. We can express the atomic Hamiltonian $H_d + H_U$ in a form in which the dependence on N_i, S_i, and S^i_z is explicitly given

$$H_d + H_U = \varepsilon_d \sum_i n_i + U \sum_i \left[-\left(S^i_z\right)^2 + \frac{n_i^2}{4} \right], \tag{10}$$

where $S^i_z = (n_{i\uparrow} - n_{i\downarrow})/2$ is the z component of the spin operator and $n_i = \sum_\sigma n_{i\sigma} = N_i$.
In the large t/U limit and at half-filling we can downfold charge fluctuations and map the Hubbard model into an effective spin model of the form

$$H_S = \frac{1}{2} \mathit{\Gamma} \sum_{\langle ii' \rangle} \left[\boldsymbol{S}_i \cdot \boldsymbol{S}_{i'} - \frac{1}{4} n_i n_{i'} \right]. \tag{11}$$

The coupling $\mathit{\Gamma}$ can be calculated by using second-order perturbation theory. For a state in which two neighbors have opposite spins, $|\uparrow,\downarrow\rangle = c^\dagger_{i\uparrow}c^\dagger_{i'\downarrow}|0\rangle$, we obtain the energy gain

$$\mathit{\Delta} E_{\uparrow\downarrow} \sim -\sum_I \langle\uparrow,\downarrow|H_T|I\rangle\langle I \left| \frac{1}{E(2) + E(0) - 2E(1)} \right| I\rangle\langle I|H_T|\uparrow,\downarrow\rangle \sim -\frac{2t^2}{U}.$$

Here $|I\rangle$ ranges over the excited states with one of the two neighboring sites doubly occupied and the other empty, $|\uparrow\downarrow,0\rangle = c^\dagger_{i\uparrow}c^\dagger_{i\downarrow}|0\rangle$, or $|0,\uparrow\downarrow\rangle = c^\dagger_{i'\uparrow}c^\dagger_{i'\downarrow}|0\rangle$; these states can be occupied via virtual hopping processes. For a state in which two neighbors have parallel spins, $|\uparrow,\uparrow\rangle = c^\dagger_{i\uparrow}c^\dagger_{i'\uparrow}|0\rangle$, no virtual hopping is possible because of the Pauli principle, and $\mathit{\Delta} E_{\uparrow\uparrow} = 0$. Thus

$$\frac{1}{2}\mathit{\Gamma} \sim (\mathit{\Delta} E_{\uparrow\uparrow} - \mathit{\Delta} E_{\uparrow\downarrow}) = \frac{1}{2}\frac{4t^2}{U}. \tag{12}$$

The exchange coupling $\mathit{\Gamma} = 4t^2/U$ is positive, i.e., antiferromagnetic.
Canonical transformations [12] provide a scheme to derive systematically the effective spin model at any perturbation order. Let us consider a unitary transformation of the Hamiltonian

$$H_S = e^{iS} H e^{-iS} = H + [iS, H] + \frac{1}{2}[iS, [iS, H]] + \ldots.$$

We search for a transformation operator which eliminates, at a given order, hopping integrals between states with a different number of doubly occupied states. To do this first we split the

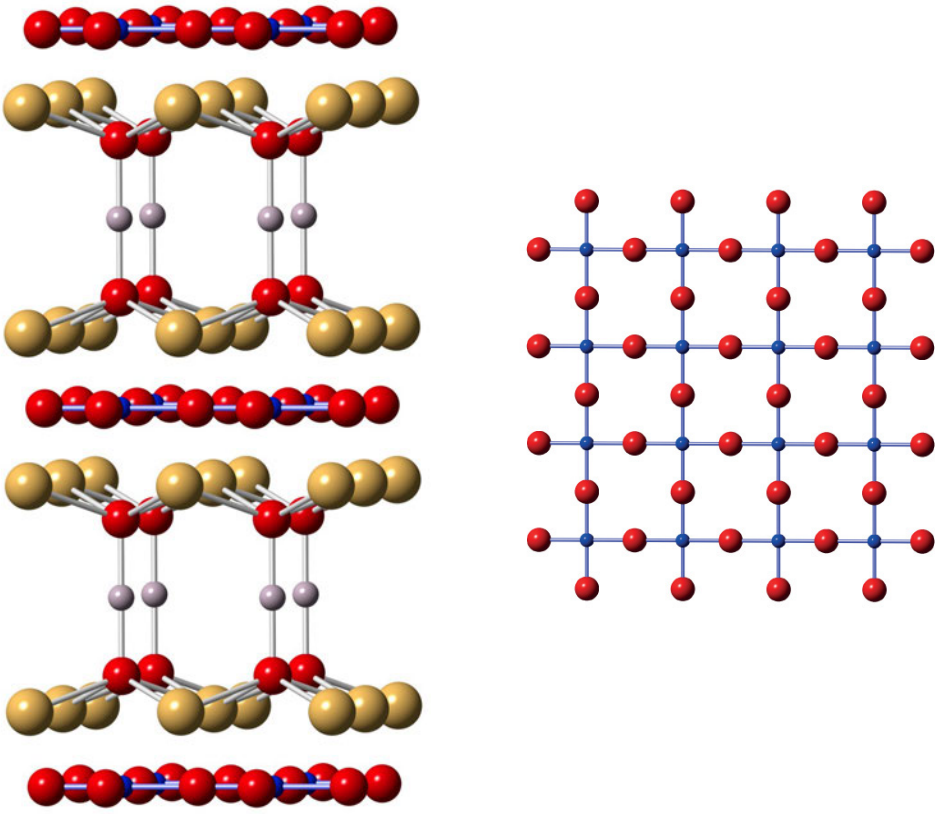

Fig. 2: *Left: The crystal structure of $HgBa_2CuO_4$ showing the two-dimensional CuO_2 layers. Spheres represent atoms of Cu (blu), O (red), Ba (yellow), and Hg (grey). Right: A CuO_2 layer. The first nearest-neighbors hopping integral between neighboring Cu sites, t, is roughly given by $\sim 4t_{pd}^2/\Delta_{dp}$, where t_{pd} is the hopping between Cu d and O p states and $\Delta_{dp} = \varepsilon_d - \varepsilon_p$ their charge-transfer energy.*

kinetic term H_T into a component, H_T^0, which does not change the number of doubly occupied states and two terms which either increase it (H_T^+) or decrease it (H_T^-) by one

$$H_T = -t \sum_{\langle ii' \rangle} \sum_{\sigma} c_{i\sigma}^{\dagger} c_{i'\sigma} = H_T^0 + H_T^+ + H_T^-,$$

where

$$\begin{aligned} H_T^0 &= -t \sum_{\langle ii' \rangle} \sum_{\sigma} n_{i-\sigma} c_{i\sigma}^{\dagger} c_{i'\sigma} n_{i'-\sigma} \\ &\quad -t \sum_{\langle ii' \rangle} \sum_{\sigma} \left(1 - n_{i-\sigma}\right) c_{i\sigma}^{\dagger} c_{i'\sigma} \left(1 - n_{i'-\sigma}\right), \\ H_T^+ &= -t \sum_{\langle ii' \rangle} \sum_{\sigma} n_{i-\sigma} c_{i\sigma}^{\dagger} c_{i'\sigma} \left(1 - n_{i'-\sigma}\right), \\ H_T^- &= \left(H_T^+\right)^{\dagger}. \end{aligned}$$

The term H_T^0 commutes with H_U. The remaining two terms fulfill the commutation rules

$$[H_T^{\pm}, H_U] = \mp U H_T^{\pm}.$$

The operator S can be expressed as a linear combination of powers of the three operators H_T^0, H_T^+, and H_T^-. The actual combination which gives the effective spin model at a given order can be found via a recursive procedure [12]. At half-filling and second order, however, we can simply guess the form of S which leads to the Hamiltonian (11). By defining

$$S = -\frac{i}{U}\left(H_T^+ - H_T^-\right)$$

we obtain

$$H_S \;=\; H_U + H_T^0 + \frac{1}{U}\left\{\left[H_T^+, H_T^-\right] + \left[H_T^0, H_T^-\right] + \left[H_T^+, H_T^0\right]\right\} + O(U^{-2}).$$

If we restrict the Hilbert space of H_S to the subspace with one electron per site (half filling), no hopping is possible without increasing the number of occupied states; hence, only the term $H_T^- H_T^+$ contributes. After some algebra, we obtain $H_S = H_S^{(2)} + O(U^{-2})$ with

$$H_S^{(2)} \;=\; \frac{1}{2}\frac{4t^2}{U}\sum_{ii'}\left[\boldsymbol{S}_i \cdot \boldsymbol{S}_{i'} - \frac{1}{4} n_i n_{i'}\right].$$

The Hubbard model (7) is seldom realized in Nature in this form. To understand real materials one typically has to take into account orbital degrees of freedom, long-range hopping integrals and sometimes longer range Coulomb interactions or perhaps even more complex many-body terms. Nevertheless, there are very interesting systems whose low-energy properties are, in the first approximation, described by (7). These are strongly correlated organic crystals (one-dimensional case) and high-temperature superconducting cuprates, in short HTSCs (two-dimensional case). An example of HTSC is $HgBa_2CuO_4$, whose structure is shown in Fig. 2. It is made of CuO_2 planes well divided by BaO-Hg-BaO blocks. The $x^2 - y^2$-like states stemming from the CuO_2 planes can be described via a one-band Hubbard model. The presence of a $x^2 - y^2$-like band at the Fermi level is a common feature of all HTSCs.

2.1 Itinerant magnetism

2.1.1 Pauli paramagnetism

Let us consider first the non-interacting limit of the Hubbard model, Hamiltonian (8). In the presence of an external magnetic field $\boldsymbol{h} = h_z \hat{z}$ the energy $\varepsilon_{\boldsymbol{k}}$ of a Bloch state is modified by the Zeeman interaction (4) as follows

$$\varepsilon_{\boldsymbol{k}} \to \varepsilon_{\boldsymbol{k}\sigma} = \varepsilon_{\boldsymbol{k}} + \frac{1}{2}\sigma g \mu_B h_z,$$

where we take the direction of the magnetic field as quantization axis and where on the right-hand side $\sigma = 1$ or -1 depending if the spin is parallel or antiparallel to $\boldsymbol{h}$. Thus, at linear order in the magnetic field, the $T = 0$ magnetization of the system is

$$M_z = -\frac{1}{2}(g\mu_B)\frac{1}{N_{\boldsymbol{k}}}\sum_{\boldsymbol{k}}\left[n_{\boldsymbol{k}\uparrow} - n_{\boldsymbol{k}\downarrow}\right] \sim \frac{1}{4}\left(g\mu_B\right)^2 \rho(\varepsilon_F) h_z,$$

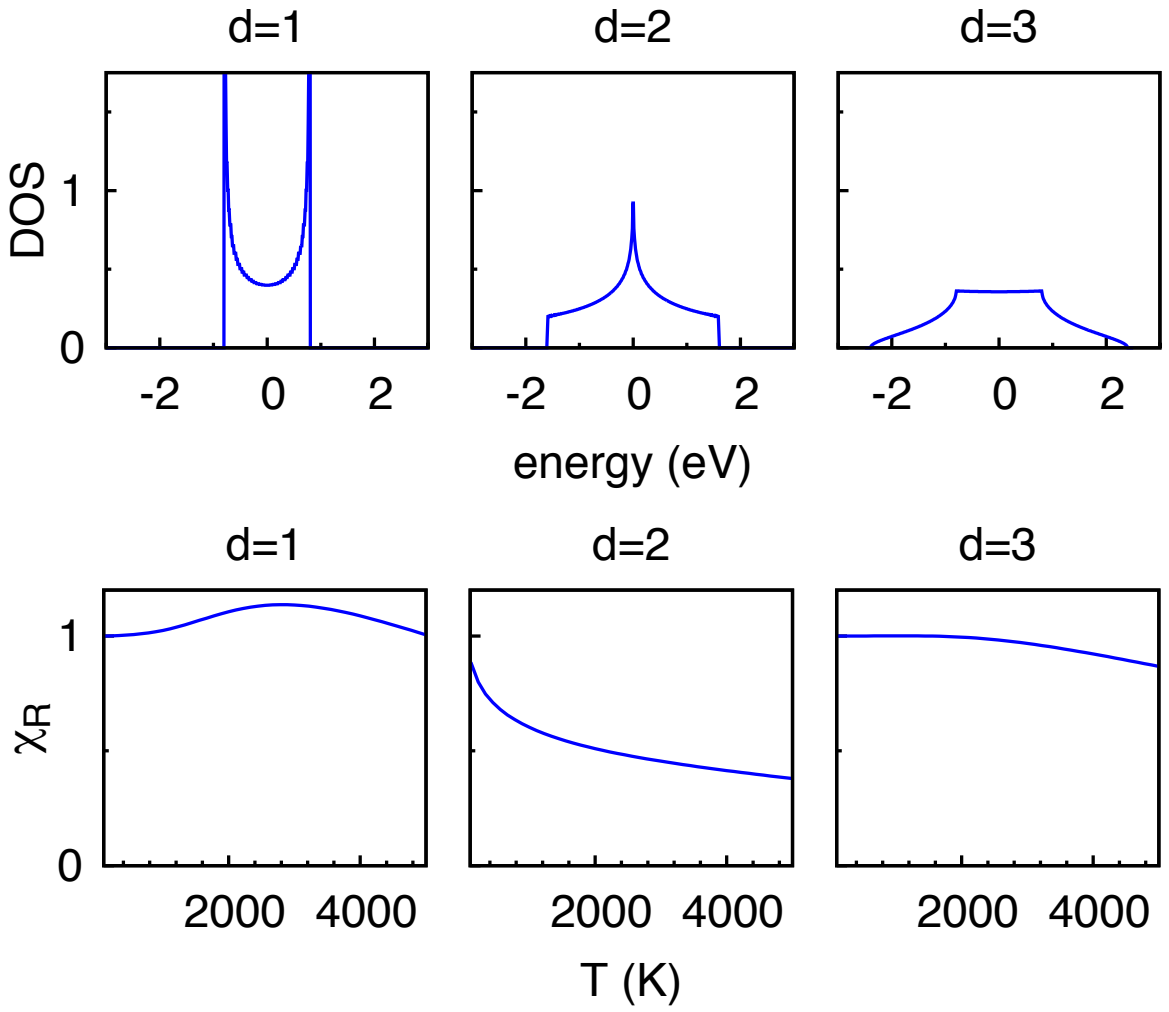

Fig. 3: *Top: Density of states (DOS) per spin, $\rho(\varepsilon)/2$, for a hypercubic lattice in one, two, and three dimension. The energy dispersion is calculated for $t = 0.4$ eV. The curves exhibit different types of Van-Hove singularities. Bottom: Effects of $\rho(\varepsilon_F)$ on the temperature dependence of $\chi_R = \chi^P(T)/\chi^P(0)$. Up to $\sim$ 1000 K only the logarithmic Van-Hove singularity (two-dimensional case) yields a sizable effect.*

where $n_{\boldsymbol{k}\sigma} = c^\dagger_{\boldsymbol{k}\sigma} c_{\boldsymbol{k}\sigma}$ and $N_{\boldsymbol{k}}$ is the number of $\boldsymbol{k}$ points; $\rho(\varepsilon_F)$ is the total density of states (DOS) at the Fermi level, ε_F. The $T = 0$ susceptibility is then given by the Pauli formula

$$\chi^P(0) = \frac{1}{4}\,(g\mu_B)^2\,\rho(\varepsilon_F).$$

In linear-response theory (see Appendix) the magnetization induced along $\hat{z}$ by an external magnetic field $h_z(\boldsymbol{q};\omega)\hat{z}$ oscillating with vector $\boldsymbol{q}$ is given by

$$M_z(\boldsymbol{q};\omega) = \chi_{zz}(\boldsymbol{q};\omega) h_z(\boldsymbol{q};\omega).$$

The Pauli susceptibility $\chi^P(0)$ is thus the static ($\omega = 0$) and uniform ($\boldsymbol{q} = \boldsymbol{0}$) linear response function to an external magnetic field. At finite temperature the Pauli susceptibility takes the

form

$$\chi^P(T) = \frac{1}{4}\left(g\mu_B\right)^2 \int d\varepsilon \rho(\varepsilon) \left(-\frac{dn(\varepsilon)}{d\varepsilon}\right),$$

where $n(\varepsilon) = 1/(1+e^{(\varepsilon-\mu)\beta})$ is the Fermi distribution function, $\beta = 1/k_B T$ and μ the chemical potential. $\chi^P(T)$ depends weakly on the temperature; its temperature dependence is more pronounced, however, in the presence of van-Hove singularities close to the Fermi level (Fig. 3). Although we have considered here the non-interacting limit of the Hubbard model, Pauli paramagnetism is important even in the $U \neq 0$ case. This happens in the so-called *Fermi-liquid* regime. When Landau Fermi-liquid theory holds there is a one-to-one correspondence between the one-electron states and the excitations of the many-body system, the *quasi particles*. The latter are characterized by heavy masses m^*

$$\frac{m^*}{m} = 1 + \frac{1}{3}F_1^s > 1, \qquad F_1^s > 0$$

and are more polarizable than electrons; correspondingly the system exhibits an enhanced Pauli susceptibility

$$\frac{\chi}{\chi^P} = \frac{1}{1+F_0^a} > 1, \qquad F_0^a < 0.$$

The coefficients F_1^s and F_0^a are Landau parameters. Because of the finite lifetime of quasiparticles and/or non Fermi-liquid phenomena of various nature, the temperature and energy regime in which the Fermi-liquid behavior is observed can be very narrow. This happens, e.g., for heavy Fermions or Kondo systems. We will discuss this in the last section.

2.1.2 Stoner instabilities

In the presence of the Coulomb interaction $U \neq 0$ finding the solution of the Hubbard model requires many-body techniques. Nevertheless, in the small U limit, we can already learn a lot about magnetism from Hartree-Fock (HF) static mean-field theory. In the simplest version of the HF approximation we make the following substitution

$$H_U = U\sum_i n_{i\uparrow}n_{i\downarrow} \rightarrow H_U^{\rm HF} = U\sum_i \left[n_{i\uparrow}\langle n_{i\downarrow}\rangle + \langle n_{i\uparrow}\rangle n_{i\downarrow} - \langle n_{i\uparrow}\rangle\langle n_{i\downarrow}\rangle\right].$$

This approximation transforms the Coulomb two-particle interaction into an effective single-particle interaction. Let us search for a ferromagnetic solution and set therefore

$$\langle n_{i\sigma}\rangle = n_\sigma = \frac{n}{2} + \sigma m,$$

where $m = (n_\uparrow - n_\downarrow)/2$ and $n = n_\uparrow + n_\downarrow$. It is convenient to rewrite the mean-field Coulomb energy as in (10), i.e., as a function of m, n and S_z^i

$$H_U^{\rm HF} = U\sum_i \left[-2mS_z^i + m^2 + \frac{n^2}{4}\right]. \tag{13}$$

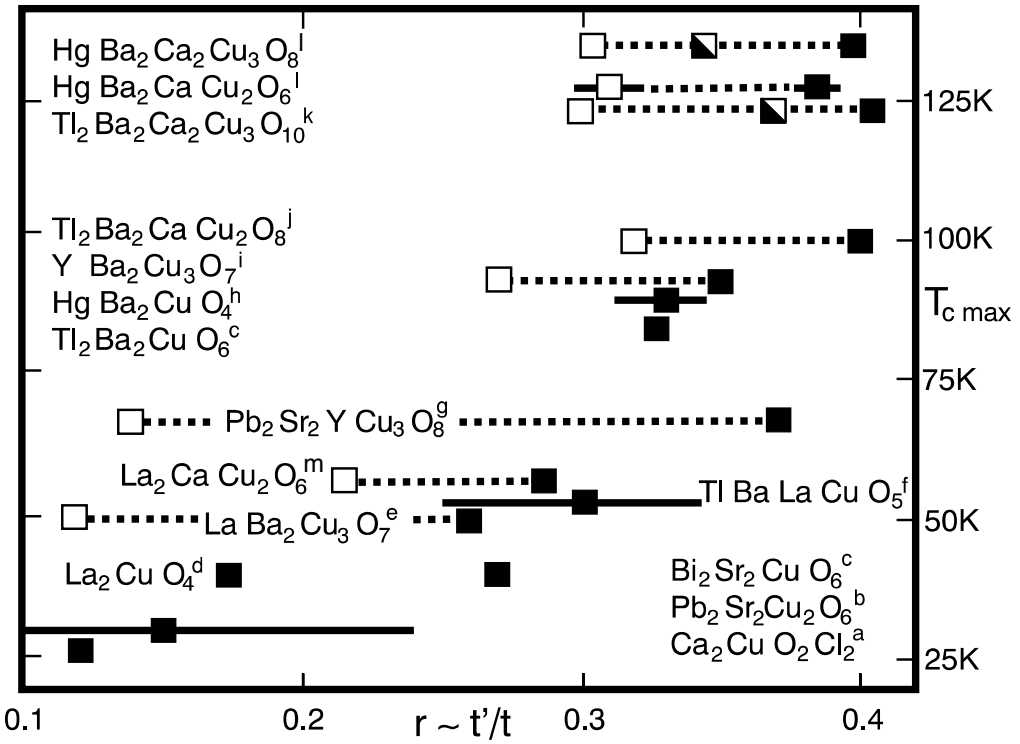

Fig. 4: *Band-structure trend in hole-doped cuprates and correlation with $T_{c\,\max}$, the maximum value of the critical temperature for superconductivity. From Ref. [13].*

The solution of the problem defined by the Hamiltonian $H_0+H_U^{\rm HF}$ amounts to the self-consistent solution of a non-interacting electron system with Bloch energies

$$\varepsilon^U_{\boldsymbol{k}\sigma} = \varepsilon_{\boldsymbol{k}} + n_{-\sigma}\,U = \varepsilon_{\boldsymbol{k}} + \frac{n}{2}U - \sigma m U.$$

In a magnetic field we additionally have to consider the Zeeman splitting. Thus

$$\varepsilon_{\boldsymbol{k}\sigma} = \varepsilon^U_{\boldsymbol{k}\sigma} + \frac{1}{2}g\mu_B h_z \sigma.$$

In the small U limit and for $T \to 0$ the magnetization $M_z = -g\mu_B m$ is then given by

$$M_z \sim \chi^P(0)\left[h_z - \frac{2}{g\mu_B}Um\right] = \chi^P(0)\left[h_z + 2(g\mu_B)^{-2}UM_z\right]$$

Solving for M_z we find the Stoner expression

$$\chi^S(\mathbf{0};0) = \frac{\chi^P(0)}{1 - 2\left(g\mu_B\right)^{-2}U\chi^P(0)}.$$

Thus with increasing U the $\boldsymbol{q} = \mathbf{0}$ static susceptibility increases and at the critical value

$$U_c = 2/\rho(\varepsilon_F)$$

it diverges, i.e., even an infinitesimal magnetic field can produce a finite magnetization. This means that the ground state becomes unstable against ferromagnetic order.

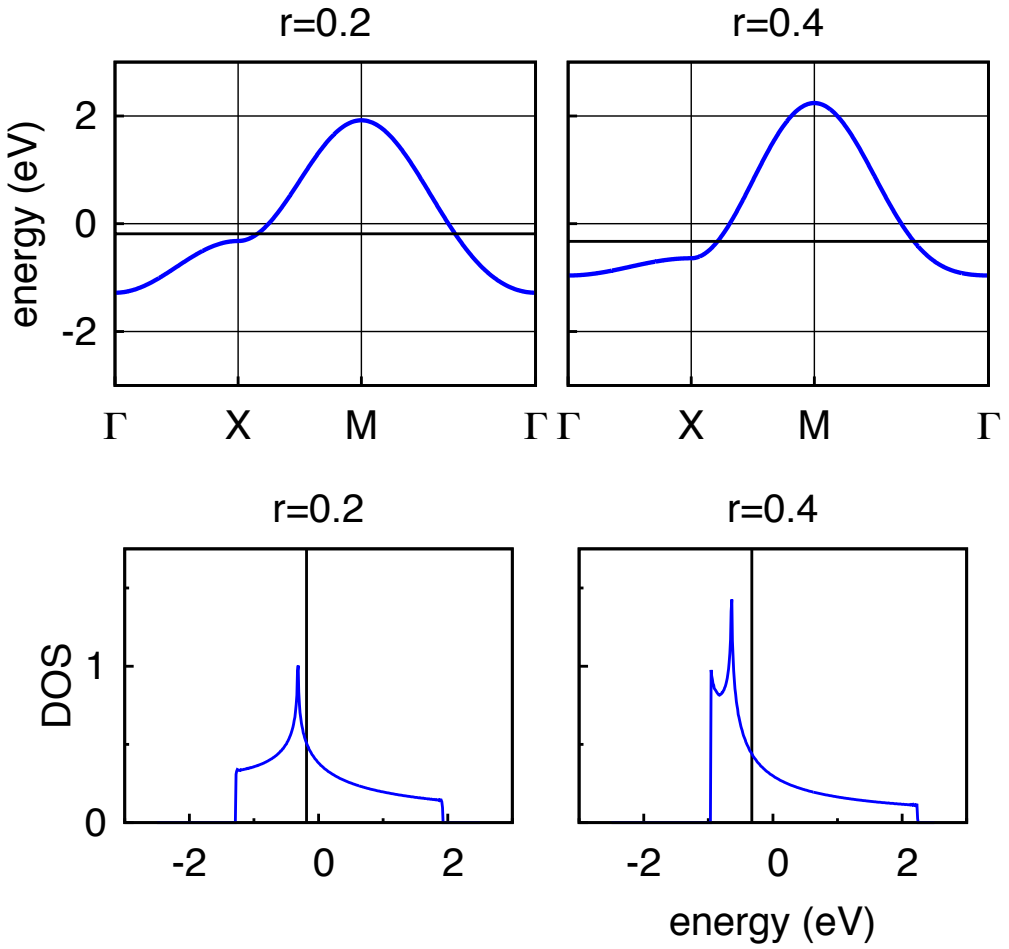

Fig. 5: *Top: Effect of $r = t'/t$ on the band structure of the two-dimensional tight-binding model. Black line: Fermi level at half filling. Bottom: corresponding density of states per spin.*

Let us consider the case of the half-filled d-dimensional hypercubic lattice whose density of states is shown in Fig. 3. In three dimensions the DOS is flat around the Fermi level, e.g., $\rho(\varepsilon_F) \sim 2/W$ where W is the band width. For a flat DOS ferromagnetic instabilities are likely only when $U \sim W$, a rather large value of U, which typically also brings in strong-correlation effects not described by static mean-field theory. In two dimensions we have a rather different situation because a logarithmic Van-Hove singularity is exactly at the Fermi level (Fig. 3); a system with such a density of states is unstable toward ferromagnetism even for very small U. In real materials distortions or long-range interactions typically push the Van-Hove singularities away from the Fermi level. In HTSCs the electronic dispersion is modified as follows by the hopping t' between second nearest neighbors

$$\varepsilon_{\boldsymbol{k}} = -2t[\cos(k_x a) + \cos(k_y a)] + 4t' \cos(k_x a)\ \cos(k_y a).$$

As shown in Fig. 4, the parameter $r \sim t'/t$ ranges typically from ~ 0.15 to 0.4 [13]. Fig. 5 shows that with increasing r the Van-Hove singularity moves downwards in energy.
It is at this point natural to ask ourselves if ferromagnetism is the only possible instability. For a given system, magnetic instabilities with $\boldsymbol{q} \neq \boldsymbol{0}$ might be energetically favorable with respect

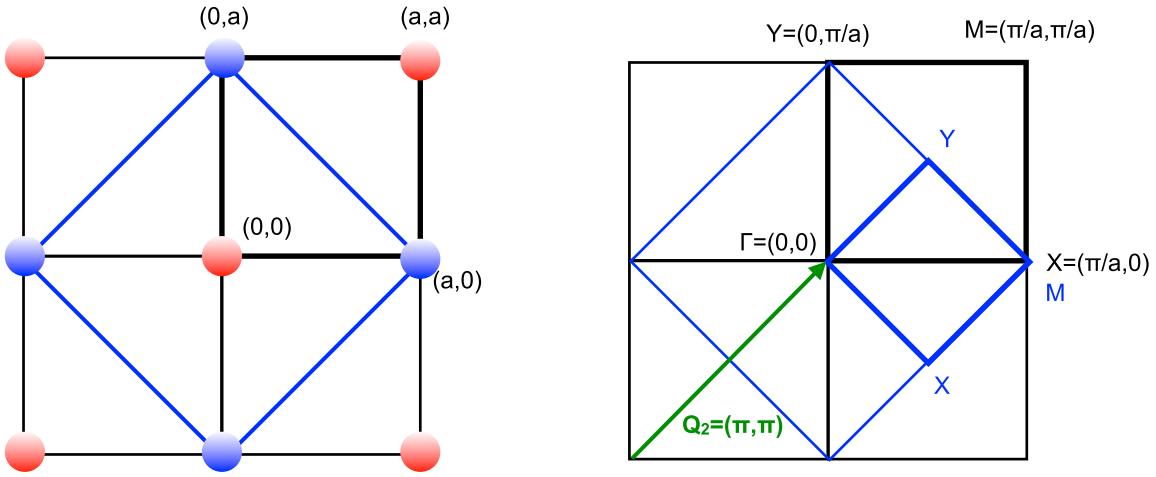

Fig. 6: *Doubling of the cell due to antiferromagnetic order and corresponding folding of the Brillouin zone (BZ) for a two-dimensional hypercubic lattice. The antiferromagnetic* $\boldsymbol{Q}_2 = (\pi/a, \pi/a, 0)$ *vector is also shown.*

to ferromagnetism; an example of a finite-$\boldsymbol{q}$ instability is antiferromagnetism (see Fig. 6). To investigate finite-$\boldsymbol{q}$ instabilities we generalize the Stoner criterion. Let us consider a magnetic excitation characterized by the vector $\boldsymbol{q}$ commensurate with the reciprocal lattice. This magnetic superstructure defines a new lattice; the associated supercell includes $j = 1, \ldots, N_j$ magnetically non-equivalent sites. We define therefore the quantities

$$\begin{aligned} S_z^i(\boldsymbol{q}) &= \sum_j e^{i\boldsymbol{q}\cdot\boldsymbol{R}_j} S_z^{ji}, \\ \langle S_z^{ji} \rangle &= m \cos(\boldsymbol{q}\cdot\boldsymbol{R}_j), \end{aligned}$$

where j runs over the magnetically non-equivalent sites $\{\boldsymbol{R}_j\}$ and i over the supercells in the lattice. In the presence of a magnetic field oscillating with vector $\boldsymbol{q}$ and pointing in the z direction, $\boldsymbol{h}_j = h_z \cos(\boldsymbol{q}\cdot\boldsymbol{R}_j)\hat{z}$, the mean-field Coulomb and Zeeman terms can be written as

$$H_U^{\mathrm{HF}} + H_Z = \sum_i \left[\frac{g\mu_B}{2} \left(h_z - \frac{2}{g\mu_B} mU \right) \left[S_z^i(\boldsymbol{q}) + S_z^i(-\boldsymbol{q}) \right] + m^2 + \frac{n^2}{4} \right],$$

where m has to be determined self-consistently. This leads to the generalized Stoner formula

$$\chi^S(\boldsymbol{q};0) = \frac{1}{2}(g\mu_B)^2 \frac{\chi_0(\boldsymbol{q};0)}{[1 - U\chi_0(\boldsymbol{q};0)]}, \tag{14}$$

$$\chi_0(\boldsymbol{q};0) = -\frac{1}{N_{\boldsymbol{k}}} \sum_{\boldsymbol{k}} \frac{n_{\boldsymbol{k}+\boldsymbol{q}} - n_{\boldsymbol{k}}}{\varepsilon_{\boldsymbol{k}+\boldsymbol{q}} - \varepsilon_{\boldsymbol{k}}}.$$

The expression (14) is the same that we can find in the so-called random-phase approximation. For $\boldsymbol{q} = \boldsymbol{0}$ in the zero-temperature limit we recover the ferromagnetic RPA susceptibility with

$$\chi_0(\boldsymbol{0};0) = 2\,(g\mu_B)^{-2}\,\chi^P(0) \sim \frac{1}{2}\rho(\varepsilon_F).$$

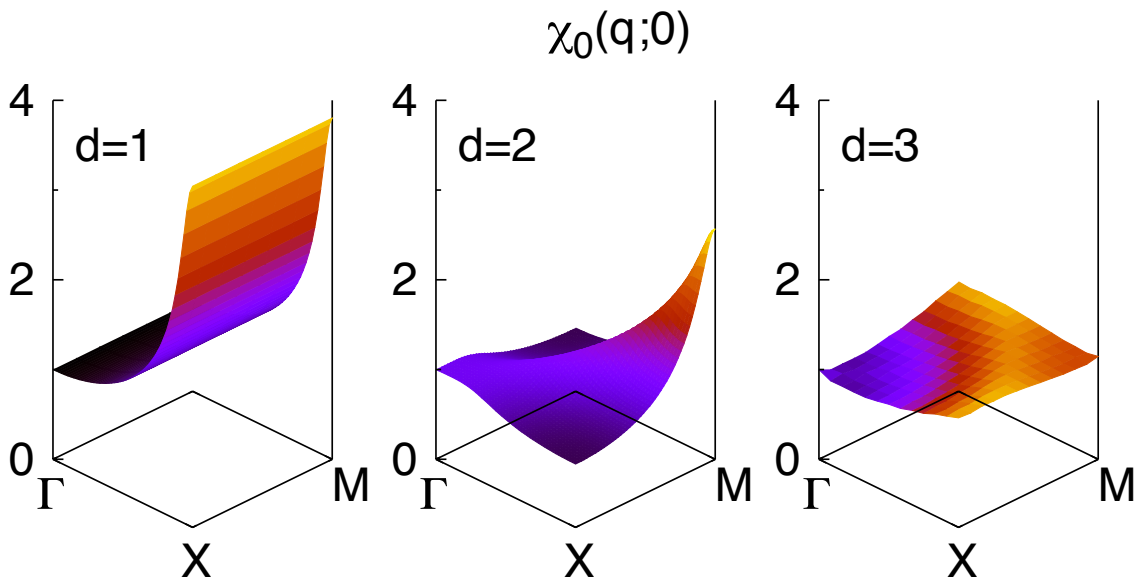

Fig. 7: *The ratio $\chi_0(\boldsymbol{q};0)/\chi_0(\boldsymbol{0};0)$ in the xy plane for a hypercubic lattice ($T \sim 230$ K) at half filling. From left to right: one, two and three dimensions.*

Figure 7 shows the non-interacting susceptibility in the xy plane for our d-dimensional hypercubic lattice. The figure shows that, in the one-dimensional case, the susceptibility diverges at the antiferromagnetic vector $\boldsymbol{Q}_1 = (\pi/a, 0, 0)$; in two dimensions this happens at $\boldsymbol{Q}_2 = (\pi/a, \pi/a, 0)$; in three dimension at $\boldsymbol{Q}_3 = (\pi/a, \pi/a, \pi/a)$, not shown in the figure. The energy dispersion exhibits at these vectors the property of perfect nesting

$$\varepsilon_{\boldsymbol{k}+\boldsymbol{Q}_i} = -\varepsilon_{\boldsymbol{k}}.$$

Remarkably, the $T = 0$ non-interacting susceptibility $\chi_0(\boldsymbol{Q}_i;0)$ diverges logarithmically at the nesting vector unless the density of states is zero at the Fermi level ($\varepsilon \to 0$)

$$\chi_0(\boldsymbol{Q}_i;0) \propto \frac{1}{4}\int_{-\infty}^{\varepsilon_F=0} d\varepsilon \rho(\varepsilon)\frac{1}{\varepsilon} \to \infty.$$

Under these conditions an arbitrary small U can cause a magnetic transition with magnetic vector $\boldsymbol{Q}_i$. In the two-dimensional case we have reached a similar conclusion for the $T = 0$ ferromagnetic ($\boldsymbol{q} = \boldsymbol{0}$) instability. The finite-temperature $\chi_0(\boldsymbol{q};0)$ susceptibility (Fig. 7) shows that, however, the antiferromagnetic instability is the strongest. Perfect nesting at $\boldsymbol{Q}_2$ is suppressed by $t' \neq 0$

$$\varepsilon_{\boldsymbol{k}+\boldsymbol{Q}_2} = -\varepsilon_{\boldsymbol{k}} + 8t' \cos(k_x a)\ \cos(k_y a).$$

Figure 8 shows how the susceptibility is modified by $t' \neq 0$ (half filling). The $\boldsymbol{Q}_2$ instability is important even for $t' \sim 0.4t$, but instabilities at incommensurate vectors around it are stronger. As a last remark it is important to notice that the RPA expression (14) depends on the filling only through the density of states, i.e., magnetic instabilities described by the Stoner formula can exist at *any* filling. This is very different from the case of the local moment regime that we will discuss starting from the next section.

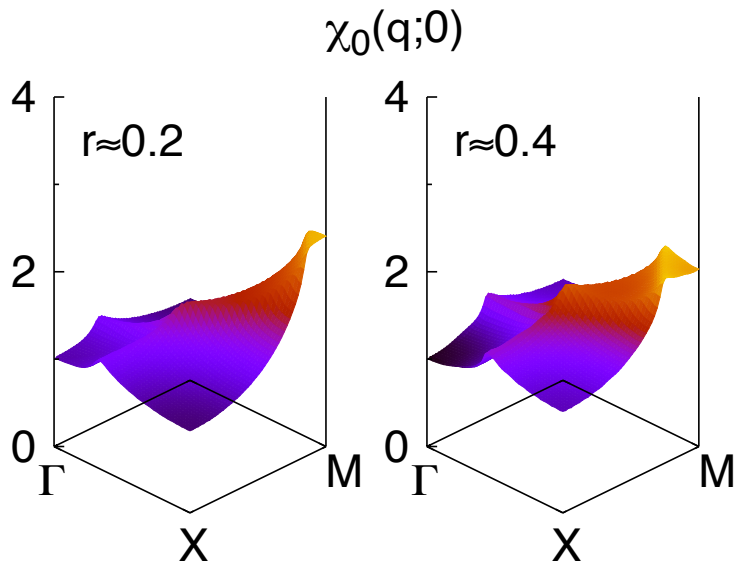

Fig. 8: *The ratio $\chi_0(\boldsymbol{q};0)/\chi_0(\mathbf{0};0)$ in the xy plane for the two-dimensional hypercubic lattice (230 K) at half filling. Left: $t' = 0.2t$. Right: $t' = 0.4t$.*

2.2 Isolated magnetic ions

2.2.1 Paramagnetism

As we have seen, the ground-state multiplet of free ions with partially occupied shells can be determined via the Hund's rules. In Tab. 1 and Tab. 2 we can find the values of the S, L, and J quantum numbers for the ground-state multiplet of the most common transition-metal and rare-earth ions. If $t = 0$ and $n = 1$, the Hubbard model (7) describes precisely a collection of idealized free ions with an incomplete shell. For such idealized ions the only possible multiplet is the one with quantum numbers $J = S = 1/2, L = 0$. In the presence of a uniform external magnetic field $h_z\hat{z}$ we can then obtain the magnetization per atom as

$$M_z = \langle M_z^i \rangle = -g\mu_B \frac{\mathrm{Tr}\,\left[e^{-g\mu_B h_z \beta S_z^i} S_z^i\right]}{\mathrm{Tr}\,\left[e^{-g\mu_B h_z \beta S_z^i}\right]} = g\mu_B S \tanh\left(g\mu_B h_z \beta S\right),$$

and thus

$$\frac{\partial M_z}{\partial h_z} = \left(g\mu_B S\right)^2 \frac{1}{k_B T}\left[1 - \tanh^2\left(g\mu_B h_z \beta S\right)\right].$$

The static uniform susceptibility is then given by the $h \to 0$ limit

$$\chi_{zz}(\mathbf{0};0) = \left(g\mu_B S\right)^2 \frac{1}{k_B T} = \frac{C_{1/2}}{T}, \tag{15}$$

where $C_{1/2}$ is the $S = 1/2$ Curie constant. If $S = 1/2$, the relation $S^2 = S(S+1)/3$ holds. Thus, for reasons that will become clear in short, the Curie constant is typically expressed as

$$C_{1/2} = \frac{\left(g\mu_B\right)^2 S(S+1)}{3k_B}.$$

Ion			n	S	L	J	$^{2S+1}L_J$
V^{4+}	Ti^{3+}		$3d^1$	1/2	2	3/2	$^2D_{3/2}$
	V^{3+}		$3d^2$	1	3	2	$^2F_2$
	Cr^{3+}	V^{2+}	$3d^3$	3/2	3	3/2	$^4F_{3/2}$
	Mn^{3+}	Cr^{2+}	$3d^4$	2	2	0	$^5D_0$
	Fe^{3+}	Mn^{2+}	$3d^5$	5/2	0	5/2	$^6S_{5/2}$
		Fe^{2+}	$3d^6$	2	2	4	$^5D_4$
		Co^{2+}	$3d^7$	3/2	3	9/2	$^4F_{9/2}$
		Ni^{2+}	$3d^8$	1	3	4	$^3F_4$
		Cu^{2+}	$3d^9$	1/2	2	5/2	$^2D_{5/2}$

Table 1: *Quantum numbers of the ground-state multiplet for several transition-metal ions with partially filled d shells. In transition-metal oxides the angular momentum is typically quenched because of the crystal-field and therefore only the total spin matters.*

If the ions have ground-state total angular momentum J we can calculate the susceptibility with the same technique, provided that we replace g with the Landé factor g_J

$$\begin{aligned} g_J &= \frac{\langle JJ_zLS|(g\boldsymbol{S}+\boldsymbol{L})\cdot\boldsymbol{J}|JJ_zLS\rangle}{\langle JJ_zLS|\boldsymbol{J}\cdot\boldsymbol{J}|JJ_zLS\rangle} \\ &\sim \frac{3}{2}+\frac{S(S+1)-L(L+1)}{2J(J+1)}, \end{aligned}$$

and calculate the thermal average of the magnetization, $\boldsymbol{M} = -g_J\mu_B\boldsymbol{J}$, accounting for the $2J+1$ degeneracy of the multiplet. The result is

$$M_z = \langle M_z^i\rangle = g_J\mu_B J\, B_J\left(g_J\mu_B h_z\beta J\right)$$

where $B_J(x)$ is the Brillouin function

$$B_J(x) = \frac{2J+1}{2J}\coth\left(\frac{2J+1}{2J}x\right) - \frac{1}{2J}\coth\left(\frac{1}{2J}x\right).$$

In the low-temperature ($x\to\infty$) limit $B_J(x)\sim 1$, and thus the magnetization approaches its saturation value in which all atoms are in the ground state

$$M_z \sim g_J\mu_B J \equiv M_0.$$

In the high-temperature ($x\to 0$) limit

$$B_J(x) \sim x\,\frac{J+1}{3J}\left[1-\frac{2J^2+2J+1}{30J^2}x^2\right],$$

and thus the susceptibility exhibits the Curie high-temperature behavior

$$\chi_{zz}(\mathbf{0};0) \sim \frac{C_J}{T} = \frac{\mu^2}{3k_BT},$$

Ion	n	S	L	J	$^{2S+1}L_J$	g_J
Ce^{3+}	$4f^1$	1/2	3	5/2	$^2F_{5/2}$	6/7
Pr^{3+}	$4f^2$	1	5	4	$^3H_4$	4/5
Nd^{3+}	$4f^3$	3/2	6	9/2	$^4I_{9/2}$	8/11
Pm^{3+}	$4f^4$	2	6	4	$^5I_4$	3/5
Sm^{3+}	$4f^5$	5/2	5	5/2	$^6H_{5/2}$	2/7
Eu^{3+}	$4f^6$	3	3	0	$^7F_0$	0
Gd^{3+}	$4f^7$	7/2	0	7/2	$^8S_{7/2}$	2
Tb^{3+}	$4f^8$	3	3	6	$^7F_6$	3/2
Dy^{3+}	$4f^9$	5/2	5	15/2	$^6H_{15/2}$	4/3
Ho^{3+}	$4f^{10}$	2	6	8	$^5I_8$	5/4
Er^{3+}	$4f^{11}$	3/2	6	15/2	$^4I_{15/2}$	6/5
Tm^{3+}	$4f^{12}$	1	5	6	$^3H_6$	7/6
Yb^{3+}	$4f^{13}$	1/2	3	7/2	$^2F_{7/2}$	8/7

Table 2: *Quantum numbers of the ground-state multiplet for rare-earth ions with partially filled f shells and corresponding g_J factor. In $4f$ materials the crystal field is typically small; thus the ground-state multiplet is in first approximation close to that of the corresponding free ion.*

where the generalized Curie constant is

$$C_J \;=\; \frac{(g_J\mu_B)^2 J(J+1)}{3k_B},$$

and where $\mu = g_J\mu_B\sqrt{J(J+1)}$ is the total magnetic moment. Correspondingly, the susceptibility decreases as $1/T$ with increasing T (Fig. 9). We have thus the three limit cases

$$\chi_{zz}(\mathbf{0};0) \sim \begin{cases} 0 & k_BT/|M_0|h_z \to 0 \\ C_J/T & |M_0|h_z/k_BT \to 0 \\ C_J/T & h_z \to 0 \end{cases}.$$

Remarkably, the $T \to 0$ and $h_z \to 0$ limit cannot be interchanged. If h_z is finite the susceptibility goes to zero in the $T \to 0$ limit; instead, if we perform the $h_z \to 0$ limit first it diverges with the Curie form $1/T$. The point $h_z = T = 0$ is a critical point in the phase space.
Let us return to the $S = 1/2$ case, i.e., the one relevant for the Hubbard model. It is interesting to calculate the inter-site spin correlation function $\mathcal{S}_{i,i'}$

$$\mathcal{S}_{i,i'} \;=\; \langle(\boldsymbol{S}_i - \langle\boldsymbol{S}_i\rangle)\cdot(\boldsymbol{S}_{i'} - \langle\boldsymbol{S}_{i'}\rangle)\rangle = \langle\boldsymbol{S}_i\cdot\boldsymbol{S}_{i'}\rangle - \langle\boldsymbol{S}_i\rangle\cdot\langle\boldsymbol{S}_{i'}\rangle\,.$$

We express $\langle\boldsymbol{S}_i\cdot\boldsymbol{S}_{i'}\rangle$ in the form $[S(S+1)-S_i(S_i+1)-S_{i'}(S_{i'}+1)]/2$, where $S_i = S_{i'} = 1/2$ and $\boldsymbol{S} = \boldsymbol{S}_i + \boldsymbol{S}_{i'}$ is the total spin. Then, since in the absence of magnetic field $\langle\boldsymbol{S}_i\rangle = \langle\boldsymbol{S}_{i'}\rangle = 0$,

$$\mathcal{S}_{i,i'} = [S(S+1) - 3/2]/2 = \begin{cases} 1/4 & S = 1 \\ -3/4 & S = 0 \end{cases}.$$

The ideal paramagnetic state is however characterized by uncorrelated sites. Hence

$$\mathcal{S}_{i,i'} = \langle\boldsymbol{S}_i\cdot\boldsymbol{S}_{i'}\rangle \sim \begin{cases} \langle\boldsymbol{S}_i\rangle\cdot\langle\boldsymbol{S}_{i'}\rangle & \sim 0 \quad i \neq i' \\ \langle\boldsymbol{S}_i\cdot\boldsymbol{S}_i\rangle & = 3/4 \quad i = i' \end{cases}. \tag{16}$$

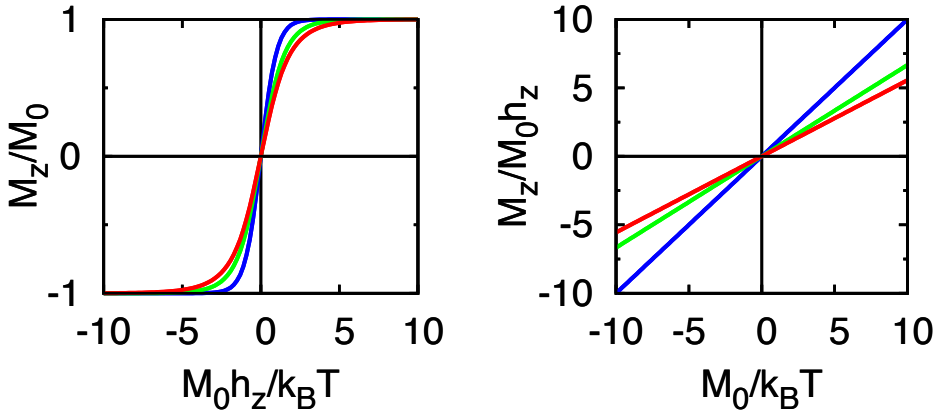

Fig. 9: *Left:* $M_z/M_0 = B_J(x)$ *as a function of* $x = h_z M_0/k_B T$. *The different lines correspond to* $J = 1/2$ *(blue),* $J = 1$ *(green) and* $J = 3/2$ *(red). Right: The ratio* $M_z/M_0 h_z$ *for finite magnetic field in the small* x *limit; the slope is* $(J+1)/3J$.

The (ideal) paramagnetic phase is thus quite different from a spatially disordered state, i.e., a situation in which each ion has a spin oriented in a given direction but spin orientations are randomly distributed. In the latter case, in general, $\langle \boldsymbol{S}^i \cdot \boldsymbol{S}^{i'} \rangle \neq 0$ for $i' \neq i$, even if, e.g., the sum of $\langle S_z^i \cdot S_z^{i'} \rangle$ over all sites i' with $i' \neq i$ is zero

$$\sum_{i' \neq i} \langle S_z^i \cdot S_z^{i'} \rangle \sim 0.$$

The high-temperature static susceptibility can be obtained from the correlation function Eq. (16) using the *fluctuation-dissipation theorem* and the Kramers-Kronig relations (see Appendix). The result is

$$\chi_{zz}(\boldsymbol{q};0) \sim \frac{(g\mu_B)^2}{k_B T} \sum_{i'} \mathcal{S}_{zz}^{i,i'} e^{i\boldsymbol{q}\cdot(\boldsymbol{R}_i - \boldsymbol{R}_{i'})} = \chi_{zz}^i(T) = \frac{M_0^2}{k_B T} = \frac{C_{1/2}}{T}. \tag{17}$$

This shows that $\chi_{zz}(\boldsymbol{q};0)$ is $\boldsymbol{q}$-independent and coincides with the local susceptibility $\chi_{zz}^i(T)$

$$\chi_{zz}(\boldsymbol{0};0) = \lim_{h_z \to 0} \frac{\partial M_z}{\partial h_z} = \chi_{zz}^i(T).$$

How can the spin susceptibility (17) be obtained directly from the atomic limit of the Hubbard model, Eq. (10)? To calculate it we can use, e.g., the imaginary time and Matsubara frequencies formalism (see Appendix). Alternatively at high temperatures we can obtain it from the correlation function as we have just seen. The energy of the four atomic states are given by (9) and, at half filling, the chemical potential is $\mu = \varepsilon_d + U/2$. Therefore

$$\begin{aligned} \chi_{zz}(\boldsymbol{0};0) &\sim \frac{(g\mu_B)^2}{k_B T} \left\{ \frac{\mathrm{Tr}\left[e^{-\beta(H_i - \mu N_i)} \ (S_z^i)^2\right]}{\mathrm{Tr}\left[e^{-\beta(H_i - \mu N_i)}\right]} - \left[\frac{\mathrm{Tr}\left[e^{-\beta(H_i - \mu N_i)} \ S_z^i\right]}{\mathrm{Tr}\left[e^{-\beta(H_i - \mu N_i)}\right]} \right]^2 \right\} \\ &= \frac{C_{1/2}}{T} \frac{e^{\beta U/2}}{1 + e^{\beta U/2}}. \end{aligned}$$

Thus the susceptibility depends on the energy scale

$$U = E(N_i + 1) + E(N_i - 1) - 2E(N_i).$$

If we perform the limit $U \to \infty$ we effectively eliminate doubly occupied and empty states. In this limit we recover the expression that we found for the spin $S = 1/2$ model, Eq. (17). This is a trivial example of downfolding, in which the low-energy and high-energy sector are decoupled from the start in the Hamiltonian. In the large U limit the high-energy states are integrated out leaving the system in a magnetic $S = 1/2$ state.

2.2.2 Larmor diamagnetism and Van Vleck paramagnetism

For ions with $J = 0$ the ground-state multiplet, in short $|0\rangle$, is non-degenerate and the linear correction to the ground-state total energy due to the Zeeman term is zero; remarkably, for open-shell ions the magnetization remains nevertheless finite because of higher-order corrections. At second order there are two contributions for the ground state. The first is the Van-Vleck term

$$M_z^{\mathrm{VV}} = 2h_z\mu_B^2 \sum_I \frac{|\langle 0|(L_z + gS_z)|I\rangle|^2}{E_I - E_0},$$

where E_I is the energy of the excited state $|I\rangle$ and E_0 the energy of the ground-state multiplet. The Van-Vleck term is weakly temperature-dependent and typically small. The second term is the diamagnetic Larmor contribution

$$M_z^{\mathrm{L}} = -\frac{1}{4}h_z\langle 0|\sum_i (x_i^2 + y_i^2)|0\rangle.$$

The Larmor and Van-Vleck terms have opposite signs and typically compete with each other.

2.3 Interacting localized moments

2.3.1 Spin models

In the large U limit and at half filling we can map the Hubbard model into an effective Heisenberg model. In this section we solve the latter using static mean-field theory. In the mean-field approximation we replace the Heisenberg Hamiltonian (11) with

$$H_S^{\mathrm{MF}} = \frac{1}{2}\Gamma \sum_{\langle ii'\rangle} \left[\boldsymbol{S}_i \cdot \langle \boldsymbol{S}_{i'}\rangle + \langle \boldsymbol{S}_i\rangle \cdot \boldsymbol{S}_{i'} - \langle \boldsymbol{S}_i\rangle \cdot \langle \boldsymbol{S}_{i'}\rangle - \frac{1}{4}n_i n_{i'} \right].$$

In the presence of an external magnetic field $\boldsymbol{h}$ we add the Zeeman term and have in total

$$\begin{aligned} H &= g\mu_B \sum_i \left[\boldsymbol{S}_i \cdot (\boldsymbol{h} + \boldsymbol{h}_i^m) + \mathrm{const}\right], \\ \boldsymbol{h}_i^m &= n_{\langle ii'\rangle}\Gamma\langle \boldsymbol{S}_{i'}\rangle / g\mu_B, \end{aligned}$$

where $n_{\langle ii'\rangle}$ is the number of first nearest neighbors and $\boldsymbol{h}_i^m$ is the molecular field at site i. We define the quantization axis z as the direction of the external magnetic field, $\boldsymbol{h} = h_z\hat{z}$,

and assume that $\hat{z}$ is also the direction of the molecular field, $\boldsymbol{h}_i^m = \Delta h_z^i \hat{z}$. Since $\Gamma > 0$ and hypercubic lattices are bipartite, the likely magnetic order is two-sublattice antiferromagnetism. Thus we set $M_z^A = -g\mu_B\langle S_z^i\rangle$, $M_z^B = -g\mu_B\langle S_z^{i'}\rangle$,where A and B are the two sublattices, $i \in A$ and $i' \in B$. In the absence of an external magnetic field, the total magnetization per formula unit, $M_z = (M_z^B + M_z^A)/2$, vanishes in the antiferromagnetic state. We define therefore as order parameter $\sigma_m = 2m = (M_z^B - M_z^A)/2M_0$, which is zero only above the critical temperature for antiferromagnetic order. We then calculate the magnetization for each sublattice and find the system of coupled equations

$$\left\{ \begin{array}{rcl} M_z^A/M_0 &=& B_{1/2}\left[M_0(h_z + \Delta h_z^A)\beta\right] \\ M_z^B/M_0 &=& B_{1/2}\left[M_0(h_z + \Delta h_z^B)\beta\right] \end{array} \right. , \tag{18}$$

where

$$\left\{ \begin{array}{rl} \Delta h_z^A = & -(M_z^B/M_0)\, S^2 \Gamma n_{\langle ii'\rangle}/M_0 \\ \Delta h_z^B = & -(M_z^A/M_0)\, S^2 \Gamma n_{\langle ii'\rangle}/M_0 \end{array} \right. .$$

For $h_z = 0$ the system (18) can be reduced to the single equation

$$\sigma_m = B_{1/2}\left[\sigma_m S^2 \Gamma n_{\langle ii'\rangle}\beta\right]. \tag{19}$$

This equation has always the trivial solution $\sigma_m = 0$. Figure 10 shows that, for small enough temperatures it also has a non-trivial solution $\sigma_m \neq 0$. The order parameter σ_m equals ± 1 at zero temperature and its absolute value decreases with increasing temperature. It becomes zero for $T \geq T_{\rm N}$ with

$$k_B T_{\rm N} = \frac{S(S+1)}{3} n_{\langle ii'\rangle}\Gamma.$$

If $T \sim T_{\rm N}$ we can find the non-trivial solution by first rewriting (19) as

$$\sigma_m = B_{1/2}\left[\frac{T_{\rm N}}{T}\sigma_m\right]. \tag{20}$$

The inverse of this equation yields $T/T_{\rm N}$ as a function of σ_m

$$\frac{T}{T_{\rm N}} = \frac{\sigma_m}{B_{1/2}^{-1}\left[\sigma_m\right]}.$$

If $T \sim T_{\rm N}$ the parameter σ_m is small. We then expand the right-hand side in powers of σ_m

$$\frac{\sigma_m}{B_{1/2}^{-1}(\sigma_m)} \sim \frac{\sigma_m}{\sigma_m + \sigma_m^3/3 + \ldots} \sim 1 - \sigma_m^2/3 + \ldots.$$

This leads to the following expression

$$\sigma_m = \sqrt{3}\left(1 - \frac{T}{T_{\rm N}}\right)^{1/2},$$

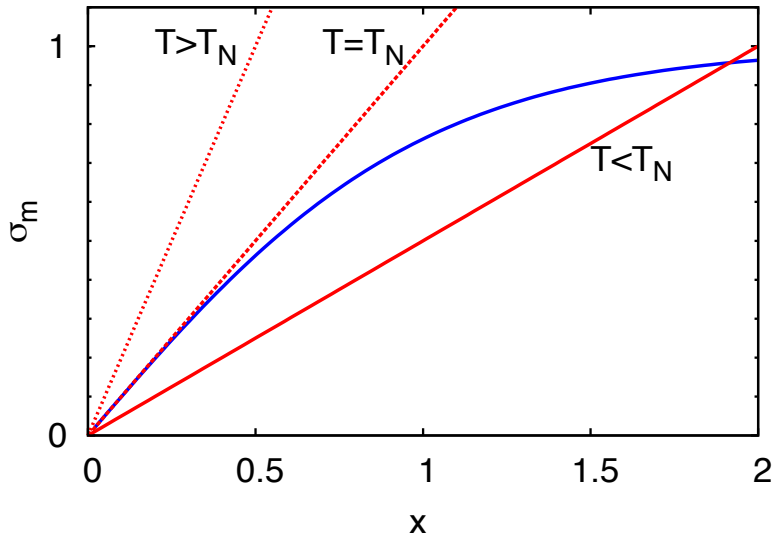

Fig. 10: *The self-consistent solution of Eq. (20) for $\sigma_m \geq 0$. The blue line shows the right-hand side of the equation, the Brillouin function $B_{1/2}(x)$, with $x = \sigma_m T_{\rm N}/T$. The red lines show the left-hand side of the equation, $\sigma_m(x) = \alpha\, x$, with $\alpha = T/T_{\rm N}$; the three different curves correspond to representative $T/T_{\rm N}$ values.*

which shows that the order parameter has a discontinuous temperature derivative at $T = T_{\rm N}$.
It is interesting to derive the expression of the static uniform susceptibility. For this we go back to the system of equations (18) and calculate from it the total magnetization M_z. In the weak magnetic field limit $M_z^A \sim -\sigma_m M_0 + \chi_{zz}(\mathbf{0};0)h_z$ and $M_z^B \sim \sigma_m M_0 + \chi_{zz}(\mathbf{0};0)h_z$. Then, by performing the first derivative of M_z with respect to h_z in the $h_z \to 0$ limit we obtain

$$\chi_{zz}(\mathbf{0};0) = \frac{C_{1/2}(1-\sigma_m^2)}{T + (1-\sigma_m^2)T_{\rm N}}.$$

The uniform susceptibility vanishes at $T = 0$ and reaches the maximum at $T = T_{\rm N}$, where it takes the value $C_{1/2}/2T_{\rm N}$. In the high-temperature regime $\sigma_m = 0$ and

$$\chi_{zz}(\mathbf{0};0) \sim \frac{C_{1/2}}{T + T_{\rm N}},$$

which is *smaller* than the susceptibility of free $S = 1/2$ magnetic ions.
The magnetic linear response is quite different if we apply an external field $\boldsymbol{h}_\perp$ perpendicular to the spins in the antiferromagnetic lattice. The associated perpendicular magnetization is

$$M_\perp \sim M_0 \frac{\sigma_m(g\mu_B h_\perp)}{\sqrt{(g\mu_B h_\perp)^2 + (4\sigma_m)^2(k_B T_{\rm N})^2}},$$

and therefore the perpendicular susceptibility is temperature-independent for $T \leq T_{\rm N}$

$$\chi_\perp(\mathbf{0};0) = \lim_{h_\perp \to 0} \frac{dM_\perp}{dh_\perp} = \frac{C_{1/2}}{2T_{\rm N}}.$$

Hence, for $T < T_{\rm N}$ the susceptibility is anisotropic, $\chi_{zz}(\mathbf{0};0) = \chi_\parallel(\mathbf{0};0) \neq \chi_\perp(\mathbf{0};0)$; at the absolute zero $\chi_\parallel(\mathbf{0};0)$ vanishes, but the response to $\boldsymbol{h}_\perp$ remains strong. For $T > T_{\rm N}$ the order parameter is zero and the susceptibility isotropic, $\chi_\parallel(\mathbf{0};0) = \chi_\perp(\mathbf{0};0)$.

We have up to now considered antiferromagnetic order only. What about other magnetic instabilities? Let us consider first ferromagnetic order. For a ferromagnetic spin arrangement by repeating the calculation we find

$$\chi_{zz}(\mathbf{0};0) = \frac{C_{1/2}(1-\sigma_m^2)}{T-(1-\sigma_m^2)T_{\rm C}},$$

where $T_C = -S(S+1)n_{\langle ii'\rangle}\Gamma/3k_B$ is, if the exchange coupling Γ is negative, the critical temperature for ferromagnetic order. Then, differently than in the antiferromagnetic case, the high-temperature uniform susceptibility is *larger* than that of free $S=1/2$ magnetic ions.
For a generic magnetic structure characterized by a vector $\boldsymbol{q}$ and a supercell with $j=1,\ldots,N_j$ magnetically non-equivalent sites we make the Ansatz

$$\langle M_z^{ji}\rangle \;=\; -\sigma_m M_0 \cos(\boldsymbol{q}\cdot\boldsymbol{R}_j) = -g\mu_B\, m\, \cos(\boldsymbol{q}\cdot\boldsymbol{R}_j)\ ,$$

where σ_m is again the order parameter. We consider a magnetic field rotating with the same $\boldsymbol{q}$ vector. By using the static mean-field approach we then find

$$k_B T_{\boldsymbol{q}} = \frac{S(S+1)}{3}\Gamma_{\boldsymbol{q}}, \quad \Gamma_{\boldsymbol{q}} = -\sum_{ij\neq 0}\Gamma^{00,ij}e^{i\boldsymbol{q}\cdot(\boldsymbol{T}_i+\boldsymbol{R}_j)}, \tag{21}$$

where $\Gamma^{00,ij}$ is the exchange coupling between the spin at the origin and the spin at site ij, and $\{\boldsymbol{T}_i\}$ are lattice vectors. In our example, $T_{\boldsymbol{0}} = T_{\rm C}$ and $T_{\boldsymbol{q}_{\rm AF}} = T_{\rm N} = -T_{\rm C}$. Thus we have

$$\chi_{zz}(\boldsymbol{q};0) = \frac{C_{1/2}(1-\sigma_m^2)}{T-(1-\sigma_m^2)T_{\boldsymbol{q}}}, \tag{22}$$

which diverges at $T=T_{\boldsymbol{q}}$. The susceptibility $\chi_{zz}(\boldsymbol{q};0)$ reflects the spatial extension of correlations, i.e., the *correlation length*, ξ; the divergence of the susceptibility at $T_{\boldsymbol{q}}$ is closely related to the divergence of ξ. To see this we calculate ξ for a hypercubic three-dimensional lattice, assuming that the system has only one instability with vector $\boldsymbol{Q}$. First we expand Eq. (21) around $\boldsymbol{Q}$ obtaining $T_{\boldsymbol{q}} \sim T_{\boldsymbol{Q}} + \alpha(\boldsymbol{q}-\boldsymbol{Q})^2 + \ldots$ and then we calculate $\chi_{zz}^{00,ji}$, the Fourier transform of Eq. (22). We find that $\chi_{zz}^{00,ji}$ decays exponentially with $r=|\boldsymbol{T}_i+\boldsymbol{R}_j|$, i.e., $\chi_{zz}^{00,ji}\propto e^{-r/\xi}/r$. The range of the correlations is $\xi\propto[T_{\boldsymbol{Q}}/(T-T_{\boldsymbol{Q}})]^{1/2}$, which becomes infinite at $T=T_{\boldsymbol{Q}}$.
It is important to notice that in principle there can be instabilities at any $\boldsymbol{q}$ vector, i.e., $\boldsymbol{q}$ does not need to be commensurate with reciprocal lattice vectors. The value of $\boldsymbol{q}$ for which $T_{\boldsymbol{q}}$ is the largest determines (within static mean-field theory) the type of magnetic order that is realized. The antiferromagnetic structure in Fig. 6 corresponds to $\boldsymbol{q}_{\rm AF} = \boldsymbol{Q}_2 = (\pi/a, \pi/a, 0)$.
In real systems the spin S is typically replaced by an *effective magnetic moment*, $\mu_{\rm eff}$, and therefore $C_{1/2}\to C_{\rm eff} = \mu_{\rm eff}^2/3k_B$. It follows that $\mu_{\rm eff}$ is the value of the product $3k_BT\chi_{zz}(\boldsymbol{q};0)$ in the high-temperature limit (here $T\gg T_{\boldsymbol{q}}$). The actual value of $\mu_{\rm eff}$ depends, as we have discussed in the introduction, on the Coulomb interaction, the spin-orbit coupling and the crystal field. In addition, the effective moment can be screened by many-body effects, as it happens for Kondo impurities; we will discuss the latter case in the last section.

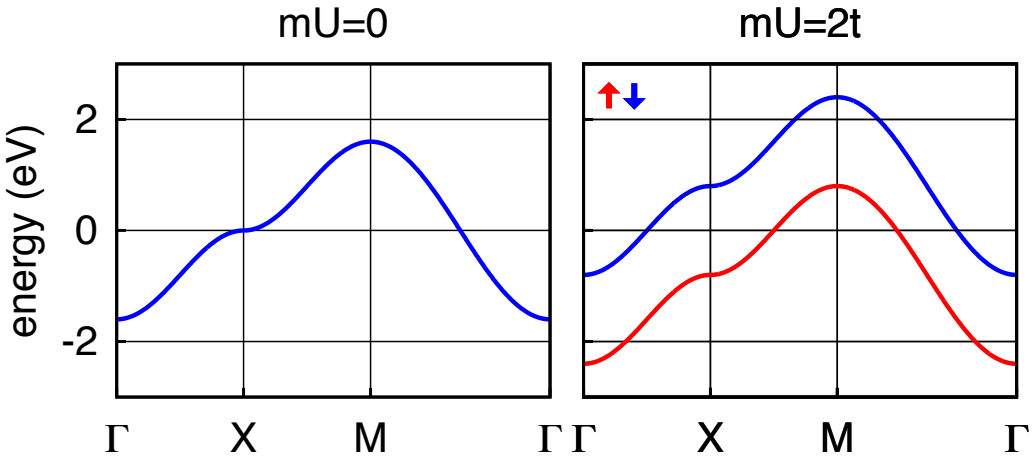

Fig. 11: *Ferromagnetism in Hartree-Fock. The chemical potential is taken as the energy zero.*

2.3.2 The Hartree-Fock approximation

We have seen that Hartree-Fock mean-field theory yields Stoner magnetic instabilities in the weak coupling limit. Can it also describe magnetism in the local moment regime ($t/U \ll 1$)? Let us focus on the half-filled two-dimensional Hubbard model for a square lattice, and let us analyze two possible magnetically ordered states, the ferro- and the antiferro-magnetic state.
If we are only interested in the ferromagnetic or the paramagnetic solution, the Hartree-Fock approximation of the Coulomb term in the Hubbard model, $H_U^{\rm HF}$, is given by Eq. (13); the HF Hamiltonian is $H = H_d + H_T + H_U^{\rm HF}$. For periodic systems it is convenient to write H in $\boldsymbol{k}$ space. We then adopt as one-electron basis the Bloch states $\Psi_{\boldsymbol{k}\sigma}$

$$\Psi_{\boldsymbol{k}\sigma}(\boldsymbol{r}) = \frac{1}{\sqrt{N_s}} \sum_i e^{i\boldsymbol{k}\cdot\boldsymbol{T}_i}\ \Psi_{i\sigma}(\boldsymbol{r}),$$

where $\Psi_{i\sigma}(\boldsymbol{r})$ is a Wannier function with spin σ, $\boldsymbol{T}_i$ a lattice vector and N_s the number of lattice sites. The term $H_U^{\rm HF}$ depends on the spin operator S_z^i, whose Fourier transform in $\boldsymbol{k}$ space is

$$S_z(\boldsymbol{k},\boldsymbol{k}') = \frac{1}{N_s} \sum_i e^{i(\boldsymbol{k}-\boldsymbol{k}')\cdot\boldsymbol{T}_i}\ \frac{1}{2} \sum_\sigma \sigma c_{i\sigma}^\dagger c_{i\sigma}.$$

The term $H_U^{\rm HF}$ has the same periodicity of the lattice and does not couple states with different $\boldsymbol{k}$ vectors. Thus only $S_z(\boldsymbol{k},\boldsymbol{k})$ contributes, and the Hamiltonian can be written as

$$H = \sum_\sigma \sum_{\boldsymbol{k}} \varepsilon_{\boldsymbol{k}} n_{\boldsymbol{k}\sigma} + U \sum_{\boldsymbol{k}} \left[-2m\ S_z(\boldsymbol{k},\boldsymbol{k}) + m^2 + \frac{n^2}{4} \right],$$

where $m = (n_\uparrow - n_\downarrow)/2$ and $n = 1$; for simplicity we set $\varepsilon_d = 0$. The HF correction splits the bands with opposite spin, leading to new one-electron eigenvalues, $\varepsilon_{\boldsymbol{k}\sigma} = \varepsilon_{\boldsymbol{k}} + \frac{1}{2}U - \sigma U m$; the chemical potential is $\mu = U/2$. The separation between $\varepsilon_{\boldsymbol{k}\uparrow} - \mu$ and $\varepsilon_{\boldsymbol{k}\downarrow} - \mu$ is $2mU$, as can be seen in Fig. 11. The system remains metallic for U smaller than the bandwidth W. In the

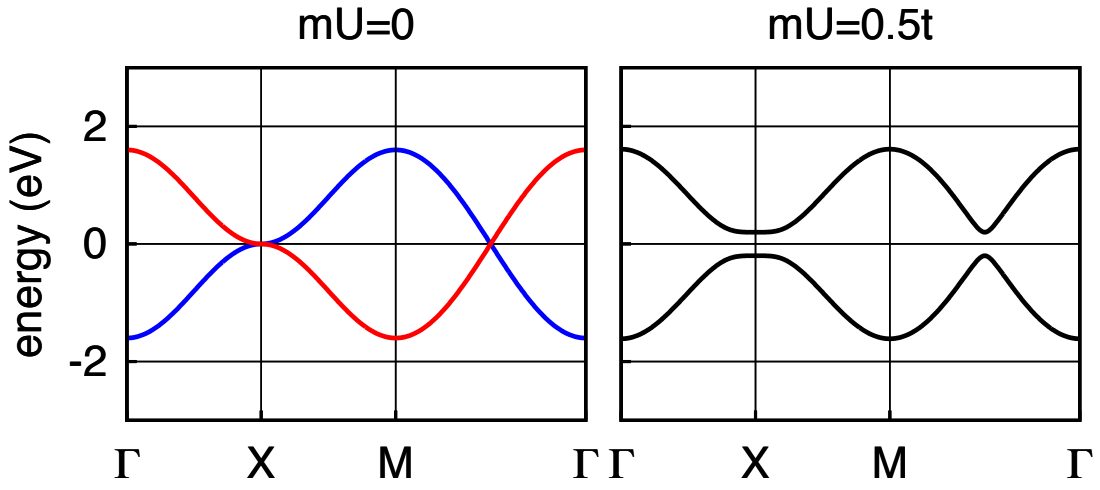

Fig. 12: *Antiferromagnetism in Hartree-Fock. The chemical potential is taken as the energy zero. Blue:* $\varepsilon_{\boldsymbol{k}}$*. Red:* $\varepsilon_{\boldsymbol{k}+\boldsymbol{Q}_2} = -\varepsilon_{\boldsymbol{k}}$*. The high-symmetry lines are those of the large BZ in Fig. 6.*

large t/U limit and at half filling we can assume that the system is a ferromagnetic insulator and $m = 1/2$. The total energy of the ground state is then

$$E_{\rm F} = \frac{1}{N_{\boldsymbol{k}}} \sum_{\boldsymbol{k}} \left[\varepsilon_{\boldsymbol{k}\sigma} - \mu\right] = \frac{1}{N_{\boldsymbol{k}}} \sum_{\boldsymbol{k}} \left[\varepsilon_{\boldsymbol{k}} - \frac{1}{2}U\right] = -\frac{1}{2}U.$$

Let us now describe the same periodic lattice via a supercell which allows for a two-sublattice antiferromagnetic solution; this supercell is shown in Fig. 6. We rewrite the Bloch states of the original lattice as

$$\Psi_{\boldsymbol{k}\sigma}(\boldsymbol{r}) \;=\; \frac{1}{\sqrt{2}}\left[\Psi^A_{\boldsymbol{k}\sigma}(\boldsymbol{r}) + \Psi^B_{\boldsymbol{k}\sigma}(\boldsymbol{r})\right], \qquad \Psi^\alpha_{\boldsymbol{k}\sigma}(\boldsymbol{r}) = \frac{1}{\sqrt{N_{s_\alpha}}} \sum_{i_\alpha} e^{i\boldsymbol{T}^\alpha_i\cdot\boldsymbol{k}}\, \Psi_{i_\alpha\sigma}(\boldsymbol{r}).$$

Here A and B are the two sublattices with opposite spins and $\boldsymbol{T}^A_i$ and $\boldsymbol{T}^B_i$ are their lattice vectors; $\alpha = A, B$. We take as one-electron basis the two Bloch functions $\Psi_{\boldsymbol{k}\sigma}$ and $\Psi_{\boldsymbol{k}+\boldsymbol{Q}_2\sigma}$, where $\boldsymbol{Q}_2 = (\pi/a, \pi/a, 0)$ is the vector associated with the antiferromagnetic instability and the corresponding folding of the Brillouin zone, also shown in Fig. 6. Then, in the HF approximation, the Coulomb interaction is given by

$$H_U^{\rm HF} = \sum_{i\in A}\left[-2mS^i_z + m^2 + \frac{n^2}{4}\right] + \sum_{i\in B}\left[+2mS^i_z + m^2 + \frac{n^2}{4}\right].$$

This interaction couples Bloch states with $\boldsymbol{k}$ vectors made equivalent by the folding of the Brillouin zone. Thus the HF Hamiltonian takes the form

$$H = \sum_{\boldsymbol{k}}\sum_{\sigma} \varepsilon_{\boldsymbol{k}} n_{\boldsymbol{k}\sigma} + \sum_{\boldsymbol{k}}\sum_{\sigma} \varepsilon_{\boldsymbol{k}+\boldsymbol{Q}_2} n_{\boldsymbol{k}+\boldsymbol{Q}_2\sigma} + U\sum_{\boldsymbol{k}}\left[-2m\; S_z(\boldsymbol{k}, \boldsymbol{k}+\boldsymbol{Q}_2) + 2m^2 + 2\frac{n^2}{4}\right].$$

The sum over $\boldsymbol{k}$ is restricted to the Brillouin zone of the antiferromagnetic lattice. We find the two-fold degenerate eigenvalues

$$\varepsilon_{\boldsymbol{k}\pm} - \mu = \frac{1}{2}(\varepsilon_{\boldsymbol{k}} + \varepsilon_{\boldsymbol{k}+\boldsymbol{Q}_2}) \pm \frac{1}{2}\sqrt{(\varepsilon_{\boldsymbol{k}} - \varepsilon_{\boldsymbol{k}+\boldsymbol{Q}_2})^2 + 4(mU)^2}. \tag{23}$$

A gap opens where the bands $\varepsilon_{\boldsymbol{k}}$ and $\varepsilon_{\boldsymbol{k}+\boldsymbol{Q}_2}$ cross, e.g., at the X point of the original Brillouin zone (Fig. 12). At half filling and for $mU = 0$ the Fermi level crosses the bands at the X point too; thus the system is insulator for any finite value of mU. In the small t/U limit we can assume that $m = 1/2$ and expand the eigenvalues in powers of $\varepsilon_{\boldsymbol{k}}/U$. For the occupied states we find

$$\varepsilon_{\boldsymbol{k}-} - \mu \sim -\frac{1}{2}U - \frac{\varepsilon_{\boldsymbol{k}}^2}{U} = -\frac{1}{2}U - \frac{4t^2}{U}\left(\frac{\varepsilon_{\boldsymbol{k}}}{2t}\right)^2$$

The ground-state total energy for the antiferromagnetic supercell is then $2E_{\rm AF}$ with

$$E_{\rm AF} = -\frac{1}{2}U - \frac{4t^2}{U}\frac{1}{N_{\boldsymbol{k}}}\sum_{\boldsymbol{k}}\left(\frac{\varepsilon_{\boldsymbol{k}}}{2t}\right)^2 \sim -\frac{1}{2}U - \frac{4t^2}{U}$$

so that the energy difference per couple of spins between ferro- and antiferro-magnetic state is

$$\Delta E^{\rm HF} = E^{\rm HF}_{\uparrow\uparrow} - E^{\rm HF}_{\uparrow\downarrow} = \frac{2}{n_{\langle ii'\rangle}}\left[E_{\rm F} - E_{\rm AF}\right] \sim \frac{1}{2}\frac{4t^2}{U} \sim \frac{1}{2}\Gamma, \tag{24}$$

which is similar to the result obtained from the Hubbard model in many-body second order perturbation theory, Eq. (12). Despite of the similarity with the actual solution, one has to remember that the spectrum of the Hartree-Fock Hamiltonian has very little to do with the spectrum of the Heisenberg model, the model which describes the actual low-energy behavior of the Hubbard Hamiltonian. If we restrict ourselves to the antiferromagnetic solution, the first excited state is at an energy $\propto U$ rather than $\propto \Gamma$; thus we cannot use a single HF calculation to understand the magnetic excitation spectrum of a given system. It is more meaningful to use HF to compare the total energy of different states and determine in this way, within HF, the ground state. Even in this case, however, one has to keep in mind that HF suffers of *spin contamination*, i.e., singlet states and $S_z = 0$ triplet states mix [11]. The energy difference per bond $E^{\rm HF}_{\uparrow\uparrow} - E^{\rm HF}_{\uparrow\downarrow}$ in Eq. (24) only resembles the exact result, as one can grasp by comparing it with the actual energy difference between triplet and singlet state in the two-site Heisenberg model

$$\Delta E = E_{S=1} - E_{S=0} = \Gamma,$$

a factor two larger. The actual ratio $\Delta E/\Delta E^{\rm HF}$ might depend on the details of the HF band structures. Thus, overall, Hartree-Fock is not the ideal approach to determine the onset of magnetic phase transitions. Other shortcomings of the Hartree-Fock approximation are in the description of the Mott metal-insulator transition. In Hartree-Fock the metal-insulator transition is intimately related to long-range magnetic order (Slater transition), but in strongly-correlated materials the metal-insulator transition can occur in the paramagnetic phase (Mott transition). It is associated with a divergence of the self-energy at low frequencies rather than with the formation of superstructures. This physics, captured by many-body methods such as the dynamical mean-field theory (DMFT) [6], is completely missed by the Hartree-Fock approximation.

3 The Kondo model

The Kondo impurity is a representative case of a system which exhibits both local moment and Pauli paramagnetic behavior, although in quite different temperature regimes [5]. The Kondo effect was first observed in diluted metallic alloys, metallic systems in which isolated d or f magnetic impurities are present, and it has been a riddle for decades. A Kondo impurity in a metallic host can be described by the Anderson model

$$H_{\rm A} = \sum_{\sigma}\sum_{\boldsymbol{k}} \varepsilon_{\boldsymbol{k}} n_{\boldsymbol{k}\sigma} + \sum_{\sigma} \varepsilon_f n_{f\sigma} + U n_{f\uparrow} n_{f\downarrow} + \sum_{\sigma}\sum_{\boldsymbol{k}} \left[V_{\boldsymbol{k}} c^\dagger_{\boldsymbol{k}\sigma} c_{f\sigma} + h.c. \right], \tag{25}$$

where ε_f is the impurity level, occupied by $n_f \sim 1$ electrons, $\varepsilon_{\boldsymbol{k}}$ is the dispersion of the metallic band and $V_{\boldsymbol{k}}$ the hybridization. If we assume that the system has particle-hole symmetry with respect to the Fermi level, then $\varepsilon_f = -U/2$. The Kondo regime is characterized by the parameters values $\varepsilon_f \ll \varepsilon_F$ and $\varepsilon_f + U \gg \varepsilon_F$, and by a weak hybridization, i.e., the hybridization function $\Delta(\varepsilon) = \pi \frac{1}{N_{\boldsymbol{k}}} \sum_{\boldsymbol{k}} |V_{\boldsymbol{k}}|^2 \delta(\varepsilon_{\boldsymbol{k}} - \varepsilon)$ is such that $\Delta(\varepsilon_F) \ll |\varepsilon_F - \varepsilon_f|, |\varepsilon_F - \varepsilon_f - U|$. Through the Schrieffer-Wolff canonical transformation [12] one can map the Anderson model onto the Kondo model[2]

$$H_{\rm K} = \sum_{\sigma}\sum_{\boldsymbol{k}} \varepsilon_{\boldsymbol{k}} n_{\boldsymbol{k}\sigma} + \Gamma \boldsymbol{S}_f \cdot \boldsymbol{s}_c(\boldsymbol{0}) = H_0 + H_\Gamma, \tag{26}$$

where

$$\Gamma \sim -2|V_{k_F}|^2 \left[\frac{1}{\varepsilon_f} - \frac{1}{\varepsilon_f + U} \right] > 0$$

is the antiferromagnetic coupling arising from the hybridization, $\boldsymbol{S}_f$ the spin of the impurity ($S_f = 1/2$), and $\boldsymbol{s}_c(\boldsymbol{0})$ is the spin-density of the conduction band at the impurity site. The solution of the problem defined by (25) or (26) is not at all trivial and requires many-body techniques such as the Wilson numerical renormalization group [14] or the Bethe Ansatz [15]. Here we only discuss some important exact results. First we define the *impurity susceptibility*, $\chi^f_{zz}(T)$, as the total susceptibility minus the contribution of the metallic band in the absence of the impurity [14–16]. One can show that at high temperatures $\chi^f_{zz}(T)$, has the following behavior

$$\chi^f_{zz}(T) \sim \frac{(g\mu_B)^2 S_f(S_f+1)}{3k_B T} \left\{ 1 - \frac{1}{\ln\left(T/T_{\rm K}\right)} \right\}.$$

This expression resembles the Curie susceptibility, apart from the $\ln(T/T_{\rm K})$ term. The scale $T_{\rm K}$ is the Kondo temperature, which, in first approximation, is given by

$$k_B T_{\rm K} \sim D e^{-2/\rho(\varepsilon_F)\Gamma},$$

[2]The Schrieffer-Wolf transformation yields additionally a potential scattering interaction, a pair tunneling coupling and a shift of the energies $\varepsilon_{\boldsymbol{k}}$. These interactions are however not important for the discussion in this section and therefore we neglect them.

where $2D = W$ is the band-width of the host conduction band. Because of the $\ln(T/T_{\rm K})$ term, the susceptibility apparently diverges at $T \sim T_{\rm K}$. In reality, however, around $T_{\rm K}$ there is a crossover to a new regime. For $T \ll T_{\rm K}$

$$\chi^f_{zz}(T) \sim \frac{C_{1/2}}{\mathcal{W}T_{\rm K}}\left\{1 - \alpha T^2 + \dots\right\},$$

where $\mathcal{W}$ is a (universal) Wilson number. Thus the low-temperature system has a Fermi-liquid behavior with enhanced density of states, i.e., with heavy masses m^*/m; furthermore $\chi^f_{zz}(0) = C_{1/2}/\mathcal{W}T_{\rm K}$ is the Curie susceptibility (Eq. (15)) with the temperature *frozen* at $T = \mathcal{W}T_{\rm K}$. At $T = 0$ the impurity magnetic moment is screened by the conduction electrons, which form a singlet state with the spin of the impurity. In other words, the effective magnetic moment formed by the impurity magnetic moment and its screening cloud,

$$\mu^2_{\rm eff}(T) \equiv 3k_BT\chi^f_{zz}(T) \propto \langle S^f_z S^f_z\rangle + \langle S^f_z s^c_z\rangle,$$

vanishes for $T \ll T_{\rm K}$. The Kondo temperature is typically 10-30 K or even smaller, hence the Fermi-liquid behavior is restricted to a very narrow energy and temperature region.

We can understand the existence of a Fermi-liquid regime by using a simple approach due to Anderson, the so-called *poor-man scaling* [17], and an argument due to Nozières. First we divide the Hilbert space into a high- and a low-energy sector. We define as *high-energy* states those with at least one electron or one hole at the top or bottom of the band; the corresponding constraint for the high-energy electronic level $\varepsilon_{\boldsymbol{q}}$ is

$$\begin{aligned} D' &< \varepsilon_{\boldsymbol{q}} < D \\ -D &< \varepsilon_{\boldsymbol{q}} < -D', \end{aligned}$$

where $D' = D - \delta D$. Next we introduce the operator P_H, which projects onto the high-energy states, and the operator $P_L = 1 - P_H$, which projects onto states with no electrons or holes in the high-energy region. Then we downfold the high-energy sector of the Hilbert space. To do this we rewrite the Kondo Hamiltonian as

$$\begin{aligned} H' &= P_LHP_L + \delta H_L = H_L + \delta H_L, \\ \delta H_L &= P_LHP_H(\omega - P_HHP_H)^{-1}P_HHP_L. \end{aligned}$$

Here H_L is the original Hamiltonian, however in the space in which the high-energy states have been eliminated; the term δH_L is a correction due to the interaction between low and (downfolded) high-energy states. Next we calculate δH_L using perturbation theory. The first non-zero contribution is of second order in Γ

$$\delta H^{(2)}_L \sim P_LH_\Gamma P_H(\omega - P_HH_0P_H)^{-1}P_HH_\Gamma P_L.$$

There are two types of processes which contribute at this order, an electron and a hole process, depending if the downfolded states have (at least) one electron or one hole in the high-energy region. Let us consider the electron process. We set

$$P_H \sim \sum_\sigma\sum_{\boldsymbol{q}} c^\dagger_{\boldsymbol{q}\sigma}|FS\rangle\langle FS|c_{\boldsymbol{q}\sigma}, \quad P_L \sim \sum_\sigma\sum_{\boldsymbol{k}} c^\dagger_{\boldsymbol{k}\sigma}|FS\rangle\langle FS|c_{\boldsymbol{k}\sigma},$$

where $|\varepsilon_{\boldsymbol{k}}| < D'$ and $|FS\rangle = \prod_{\boldsymbol{k}\sigma} c^\dagger_{\boldsymbol{k}\sigma}|0\rangle$ is the Fermi see, i.e., the many-body state corresponding to the metallic conduction band. Thus

$$\begin{aligned} \delta H_L^{(2)} &= -\frac{1}{2}\Gamma^2 \sum_{\boldsymbol{q}} \frac{1}{\omega - \varepsilon_{\boldsymbol{q}}} \boldsymbol{S}_f \cdot \boldsymbol{s}_c(\boldsymbol{0}) + \dots \\ &\sim \frac{1}{4}\rho(\varepsilon_F)\Gamma^2 \frac{\delta D}{D} \boldsymbol{S}_f \cdot \boldsymbol{s}_c(\boldsymbol{0}) + \dots . \end{aligned}$$

We find an analogous contribution from the hole process. The correction $\delta H_L^{(2)}$ modifies the parameter Γ of the Kondo Hamiltonian as follows

$$\begin{aligned} \Gamma &\rightarrow \Gamma' = \Gamma + \delta\Gamma, \\ \frac{\delta\Gamma}{\delta \ln D} &= \frac{1}{2}\rho(\varepsilon_F)\Gamma^2. \end{aligned} \tag{27}$$

The equation (27) has two fixed points, $\Gamma = 0$ (*weak coupling*) and $\Gamma \rightarrow \infty$ (*strong coupling*). By solving the scaling equations we find

$$\Gamma' = \frac{\Gamma}{1 + \frac{1}{2}\rho(\varepsilon_F)\Gamma \ln \frac{D'}{D}}.$$

If Γ is antiferromagnetic the renormalized coupling constant Γ' diverges for $D' = De^{-2/\Gamma\rho(\varepsilon_F)}$, an energy proportional to the Kondo energy $k_B T_{\rm K}$. This divergence (scaling to strong coupling) indicates that at low energy the interaction between the spins dominates and therefore the system forms a singlet in which the impurity magnetic moment is screened. The existence of this strong coupling fixed point is confirmed by the numerical renormalization group of Wilson [14]. Nozières [19] has used this conclusion to show that the low-temperature behavior of the system must be of Fermi liquid type. His argument is the following. For infinite coupling Γ' the impurity traps a conduction electron to form a singlet state. For a finite but still very large Γ' any attempt of breaking the singlet will cost a very large energy. Virtual excitations (into the $n_f = 0$ or $n_f = 2$ states and finally the $n_f = 1$ triplet state) are however possible and they yield an effective indirect interaction between the remaining conduction electrons surrounding the impurity. This is similar to the phonon-mediated attractive interaction in metals. The indirect electron-electron coupling is weak and can be calculated in perturbation theory ($1/\Gamma$ expansion). Nozières has shown that, in first approximation, the effective interaction is between electrons of opposite spins lying next to the impurity, it is of order D^4/Γ^3 and repulsive; hence it gives rise to a Fermi-liquid behavior with enhanced susceptibility [19].

If $\Gamma = \Gamma_F < 0$ (ferromagnetic coupling, as for example the coupling arising from direct Coulomb exchange) the renormalized coupling constant Γ' goes to zero in the $D' \rightarrow 0$ limit (scaling to weak coupling). This means that the local spin becomes *asymptotically free* and yields a Curie-type susceptibility, which diverges for $T \rightarrow 0$. For small but finite coupling we can account for the ferromagnetic interaction perturbatively (expansion in orders of Γ_F). In f electron materials often both ferro and antiferromagnetic exchange couplings are present, the first, Γ_F, arising from the Coulomb exchange, the second, Γ, from the hybridization. There

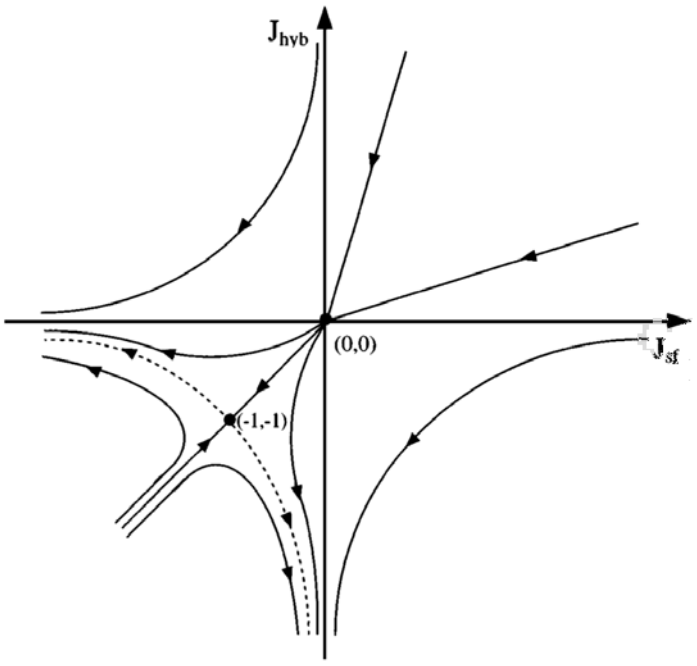

Fig. 13: *Sketch of the scaling diagrams for the two-channel Kondo model.* $\Gamma = -J_{\rm hyb}$ *and* $\Gamma_F = -J_{\rm sf}$. *For* $\Gamma > 0$ *(antiferromagnetic) and* $\Gamma_F < 0$ *(ferromagnetic) the antiferromagnetic coupling scales to strong coupling and ferromagnetic one to weak coupling (right bottom quadrant). From Ref. [18].*

are therefore two possibilities. If both exchange interactions couple the impurity with the same conduction channel, only the total coupling $\Gamma_F + \Gamma$ matters. Thus a $|\Gamma_F| > \Gamma$ suppresses the Kondo effect. If, however, ferromagnetic and antiferromagnetic exchange interaction couple the impurity to different conduction channels, a $|\Gamma_F| > \Gamma$ does not suppress the Kondo effect (Fig. 13), but merely reduces $T_{\rm K}$. In the infinite $|\Gamma_F|$ limit the model describes an undercompensated Kondo effect [18].

4 Conclusion

In this lecture we introduced some of the fundamental aspects of magnetism in correlated systems. We have seen two distinct regimes, the itinerant and the local moment regime. In the first regime we can, in most cases, treat correlation effects in perturbation theory. In the world of real materials this is the limit in which the density-functional theory (DFT), in the local-density approximation or its simple extensions, works best. If the system is weakly correlated we can calculate the linear-response function in the random-phase approximation and understand fairly well magnetism within this approach.

The opposite regime is the strong-correlation regime, in which many-body effects play a key role. In this limit perturbation theory fails and we have in principle to work with many-body methods. If, however, we are interested only in magnetic phenomena, at integer filling a strong simplification comes from mapping the original many-body Hamiltonian into an effective spin

model. The exact solution of effective spins models requires in general numerical methods such as the Monte Carlo or quantum Monte Carlo approach, or, when the system is small enough, exact diagonalization or Lanczos. These techniques are discussed in the lectures of Werner Krauth, Stefan Wessel and Jürgen Schnack. The density-matrix renormalization group (DMRG), particularly efficient for one-dimensional systems, is instead presented in the lectures of Ulrich Schollwöck and Jens Eisert.

To work with material-specific spin models we need to calculate the magnetic exchange parameters. Typically this is done starting from total-energy DFT calculations for different spin configurations, e.g., in the LDA+U approximation. The LDA+U approach is based on the Hartree-Fock approximation, and therefore when we extract the parameters from LDA+U calculations we have to keep in mind the shortcomings of the method. Furthermore if we want to extract the magnetic couplings from total energy calculations we have to make a guess on the form of the spin model. More flexible approaches, which allow us to account for actual correlations effects, are based on Green functions and the local-force theorem [20], as discussed in the lecture of Sasha Lichtenstein, or on canonical transformations [12, 21].

In strongly-correlated materials localized and itinerant moments physics can often be observed in the same system, although in different energy or temperature regimes. This is apparent in the case of the Kondo effect. For a Kondo impurity the susceptibility exhibits a Curie behavior at high temperature and a Fermi-liquid behavior at low temperature. In correlated transition-metal oxides Fermi liquid and local-spin magnetism can both play an important role but at different energy scales. Furthermore, in the absence of a large charge gap downfolding to spin models is not really justified. The modern method to bridge between localized and itinerant regime and deal with the actual complications of real systems is the dynamical mean-field theory (DMFT) [6]. Within this technique we solve directly generalized Hubbard-like models, however in the local self-energy approximation. DMFT is the first flexible approach that allows us to understand the paramagnetic Mott metal-insulator transition and thus also magnetism in correlated materials in a realistic setting. Modern DMFT codes are slowly but steadily becoming as complex and flexible as DFT codes, allowing us to deal with the full complexity of strongly-correlated materials. While this is a huge step forwards, we have to remember that state-of-the-art many-body techniques have been developed by solving simple models within certain approximations. We have to know very well these if we want to understand real materials and further advance the field. In DMFT we solve self-consistently an effective quantum-impurity model, a generalization of the Anderson model. Thus a lot can be learnt from the solution of the Anderson model in the context of the Kondo problem. Much can be understood alone with simple arguments, as Anderson or Noziéres have shown us, reaching important conclusions on the Kondo problem with paper and pencil.

Acknowledgment

Support of the Deutsche Forschungsgemeinschaft through FOR1346 is gratefully acknowledged.

Appendices

A Formalism

The formulas in this Appendix are in atomic units: The numerical value of e, m and $\hbar$ is 1, that of μ_B is 1/2, and energies are in Hartree.

A.1 Matsubara Green functions

A.1.1 Imaginary time and frequency Green functions

The imaginary time Matsubara Green function is defined as

$$G_{\alpha\beta}(\boldsymbol{\tau}) = -\langle \mathcal{T} c_\alpha(\tau_1) c^\dagger_\beta(\tau_2)\rangle = -\frac{1}{Z}\mathrm{Tr}\,\left[e^{-\beta(H-\mu N)}\mathcal{T} c_\alpha(\tau_1) c^\dagger_\beta(\tau_2)\right],$$

where $\mathcal{T}$ is the time-ordering operator, $\boldsymbol{\tau} = (\tau_1, \tau_2)$, $Z = \mathrm{Tr} e^{-\beta(H-\mu N)}$ is the partition function, and the imaginary time operators $o(\tau) = c(\tau), c^\dagger(\tau)$ are defined as $o(\tau) = e^{\tau(H-\mu N)} o\, e^{-\tau(H-\mu N)}$. The indices α and β are the flavors; they can be site and spin indices in the atomic limit, and $\boldsymbol{k}$ and spin indices in the non-interacting electrons limit. Writing explicitly the action of the time-ordering operator we obtain

$$G_{\alpha\beta}(\boldsymbol{\tau}) \;=\; -\Theta(\tau_1-\tau_2)\langle c_\alpha(\tau_1) c^\dagger_\beta(\tau_2)\rangle + \Theta(\tau_2-\tau_1)\langle c^\dagger_\beta(\tau_2) c_\alpha(\tau_1)\rangle.$$

Using the invariance of the trace of the product of operators under cyclic permutations, one can show that the following properties hold

$$\begin{aligned} G_{\alpha\beta}(\boldsymbol{\tau}) &= G_{\alpha\beta}(\tau_1-\tau_2), \\ G_{\alpha\beta}(\tau) &= -G_{\alpha\beta}(\tau+\beta) \qquad \text{for } -\beta<\tau<0. \end{aligned}$$

The Fourier transform on the Matsubara axis is

$$G_{\alpha\beta}(i\nu_n) = \frac{1}{2}\int_{-\beta}^{\beta} d\tau e^{i\nu_n\tau} G_{\alpha\beta}(\tau) = \int_0^\beta d\tau e^{i\nu_n\tau} G_{\alpha\beta}(\tau),$$

with $\nu_n = (2n+1)\pi/\beta$. The inverse Fourier transform is given by

$$G_{\alpha\beta}(\tau) = \frac{1}{\beta}\sum_{n=-\infty}^{+\infty} e^{-i\nu_n\tau} G_{\alpha\beta}(i\nu_n).$$

The convergence of $G_{\alpha\beta}(\tau)$ is only guaranteed in the interval $-\beta<\tau<\beta$. A discussion of this can be found in the lecture of Robert Eder. Finally, if n_α is the number of electrons for flavor α, one can show that

$$G_{\alpha\alpha}(\tau\to 0^+) = -1+n_\alpha, \quad G_{\alpha\alpha}(\tau\to\beta^-) = -n_\alpha. \tag{28}$$

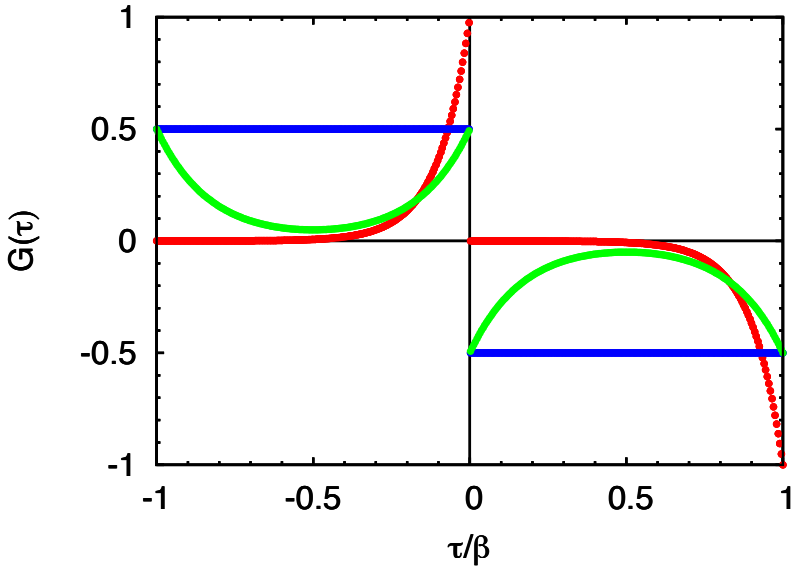

Fig. 14: *The function $\mathcal{G}_{\boldsymbol{k}\sigma}(\tau)$ defined in Eq. (30) for a state well below the Fermi level (red) and at the Fermi level (blue) and $\beta = 2$ (eV)$^{-1}$. The green line shows the atomic $G(\tau)$ from Eq. (32) for $U = 6$ eV and $h = 0$.*

A.1.2 Non-interacting limit

For a non-interacting system described by

$$H_0 = \sum_{\boldsymbol{k}} \sum_{\sigma} \varepsilon_{\boldsymbol{k}} n_{\boldsymbol{k}\sigma} \tag{29}$$

we can show that

$$\begin{aligned} \mathcal{G}_{\boldsymbol{k}\sigma}(\tau) &= -\langle \mathcal{T} \left[c_{\boldsymbol{k}\sigma}(\tau) c^{\dagger}_{\boldsymbol{k}\sigma}(0) \right] \rangle \\ &= -\left[\Theta(\tau) \left(1 - n_\sigma(\varepsilon_{\boldsymbol{k}})\right) - \Theta(-\tau) n_\sigma(\varepsilon_{\boldsymbol{k}}) \right] e^{-(\varepsilon_{\boldsymbol{k}} - \mu)\tau}, \end{aligned} \tag{30}$$

where

$$n_\sigma(\varepsilon_{\boldsymbol{k}}) = \frac{1}{1 + e^{\beta(\varepsilon_{\boldsymbol{k}} - \mu)}}.$$

The Fourier transform at Matsubara frequencies is

$$\mathcal{G}_{\boldsymbol{k}\sigma}(i\nu_n) = \frac{1}{i\nu_n - (\varepsilon_{\boldsymbol{k}} - \mu)}.$$

To obtain the analytic continuation of this Green function on the real axis we substitute

$$i\nu_n \to \omega + i0^+.$$

A.1.3 Matsubara sums

The non-interacting Green function $\mathcal{G}_{\boldsymbol{k}\sigma}(z)$ has a pole at $z_p = \varepsilon_{\boldsymbol{k}} - \mu$; the Fermi function $n_\sigma(z)$ has instead poles for $z = i\nu_n$. Let us consider the integral

$$\frac{1}{2\pi i} \oint_C \mathcal{F}_{\boldsymbol{k}\sigma}(z) n_\sigma(z) e^{z\tau} dz = 0,$$

where $0 < \tau < \beta$ and where the function $\mathcal{F}_{\boldsymbol{k}\sigma}(z)$ is analytic everywhere except at some poles $\{z_p\}$. The contour C is a circle in full complex plane centered at the origin and including the poles of the Fermi function (Matsubara frequencies) and the poles of $\mathcal{F}_{\boldsymbol{k}\sigma}(z)$. The integral is zero because the integrand vanishes exponentially for $|z| \to \infty$. Furthermore

$$\text{Res } [n_\sigma(i\nu_n)] = -\frac{1}{\beta}.$$

Using Cauchy's integral theorem we then have

$$\frac{1}{\beta}\sum_n e^{i\nu_n\tau}\mathcal{F}_{\boldsymbol{k}\sigma}(i\nu_n) = \sum_{z_p} \text{Res } [\mathcal{F}_{\boldsymbol{k}\sigma}(z_p)]\, n_\sigma(z_p)e^{z_p\tau}.$$

We can use this expression and (28) to show that

$$\begin{aligned}
\frac{1}{\beta}\sum_n e^{-i\nu_n 0^-}\mathcal{G}_{\boldsymbol{k}\sigma}(i\nu_n) &= \mathcal{G}_{\boldsymbol{k}\sigma}(0^-) = n_\sigma(\varepsilon_{\boldsymbol{k}}), \\
\frac{1}{\beta}\sum_n e^{-i\nu_n 0^+}\mathcal{G}_{\boldsymbol{k}\sigma}(i\nu_n) &= \mathcal{G}_{\boldsymbol{k}\sigma}(0^+) = n_\sigma(\varepsilon_{\boldsymbol{k}}) - 1.
\end{aligned}$$

In a similar way we can show that

$$\frac{1}{\beta}\sum_n e^{i\nu_n 0^+}\mathcal{G}_{\boldsymbol{k}\sigma}(i\nu_n)\mathcal{G}_{\boldsymbol{k}\sigma}(i\nu_n) = \frac{dn_\sigma(\varepsilon_{\boldsymbol{k}})}{d\varepsilon_{\boldsymbol{k}}} = \beta n_\sigma(\varepsilon_{\boldsymbol{k}})[-1 + n_\sigma(\varepsilon_{\boldsymbol{k}})],$$

$$\frac{1}{\beta}\sum_n e^{i\nu_n 0^+}\mathcal{G}_{\boldsymbol{k}\sigma}(i\nu_n)\mathcal{G}_{\boldsymbol{k}+\boldsymbol{q}\sigma}(i\nu_n + i\omega_m) = \frac{n_{\boldsymbol{k}+\boldsymbol{q}} - n_{\boldsymbol{k}}}{i\omega_m + \varepsilon_{\boldsymbol{k}+\boldsymbol{q}} - \varepsilon_{\boldsymbol{k}}},$$

where in the last relation $\omega_m = 2m\pi/\beta$ is a Bosonic Matsubara frequency.

A.1.4 Atomic limit

It is interesting to consider a half-filled idealized atom described by the Hamiltonian

$$H = \varepsilon_d \sum_\sigma n_\sigma + U\left(\frac{N^2}{4} - S_z^2\right) + g\mu_B h S_z. \tag{31}$$

For $\tau > 0$ we can calculate explicitly the Green function obtaining

$$G_\sigma(\tau) = -\frac{1}{2}\frac{1}{1 + e^{\beta U/2}\cosh(\beta g\mu_B h/2)}\left[e^{\tau(U - g\mu_B h\sigma)/2} + e^{(\beta-\tau)(U+g\mu_B h\sigma)/2}\right]. \tag{32}$$

The Fourier transform of $G_\sigma(\tau)$ is

$$G_\sigma(i\nu_n) = \left[\frac{w_-}{i\nu_n + (U - g\mu_B h\sigma)/2} + \frac{w_+}{i\nu_n - (U + g\mu_B h\sigma)/2}\right],$$

where

$$w_\pm = \frac{1}{2}\frac{1 + e^{\beta U/2}e^{\pm\beta g\mu_B h\sigma/2}}{1 + e^{\beta U/2}\cosh(\beta g\mu_B h/2)}.$$

Since the Green function is written as the sum of functions with one pole, the analytic continuation is simple, as in the non-interacting case. We replace $i\nu_n$ with $\omega + i0^+$.

A.1.5 Lehmann representation

Using the Lehmann representation we can rewrite

$$G_{\boldsymbol{k}\sigma}(i\nu_n) = \int A_{\boldsymbol{k}\sigma}(\varepsilon)\frac{1}{i\nu_n - \varepsilon}\, d\varepsilon,$$

where $A_{\boldsymbol{k}\sigma}(\varepsilon) = -\frac{1}{\pi}\mathrm{Im}\left[G_{\boldsymbol{k}\sigma}(\varepsilon)\right]$ is the spectral function. The spectral function is related to the density of states as follows

$$\rho_\sigma(\varepsilon) = \frac{1}{N_{\boldsymbol{k}}}\sum_{\boldsymbol{k}} A_{\boldsymbol{k}\sigma}(\varepsilon).$$

A.2 Linear response theory

A.2.1 Theory

The response of a system described by the Hamiltonian H to a small magnetic field $\boldsymbol{h}(\boldsymbol{r},t)$ is given by the linear correction to the Hamiltonian, i.e.,

$$\sum_\nu \delta H_\nu(\boldsymbol{r};t) = -\sum_\nu M_\nu(\boldsymbol{r};t)h_\nu(\boldsymbol{r};t), \tag{33}$$

where $\boldsymbol{M}(\boldsymbol{r};t)$ is the magnetization operator in the Heisenberg representation

$$M_\nu(\boldsymbol{r};t) = e^{iHt}M_\nu(\boldsymbol{r})e^{-iHt}$$

and $\nu = x,y,z$. To linear order in the perturbation, and assuming that the perturbation is turned on adiabatically at $t_0 = -\infty$

$$\langle M_\nu(\boldsymbol{r};t)\rangle = \langle M_\nu(\boldsymbol{r})\rangle_0 - i\sum_{\nu'}\int d\boldsymbol{r}' \int_{-\infty}^{t} dt' \langle [M_\nu(\boldsymbol{r};t), \delta H_{\nu'}(\boldsymbol{r}';t')]\rangle_0,$$

where $\langle M_\nu(\boldsymbol{r})\rangle_0$ is the (equilibrium) thermal average in the absence of the perturbation. By replacing $\sum_{\nu'}\delta H_{\nu'}(\boldsymbol{r}';t')$ with the expression (33) we obtain

$$\delta\langle M_\nu(\boldsymbol{r};t)\rangle = \langle M_\nu(\boldsymbol{r};t)\rangle - \langle M_\nu(\boldsymbol{r})\rangle_0 = i\sum_{\nu'}\int d\boldsymbol{r}' \int_{-\infty}^{t} dt' \langle [M_\nu(\boldsymbol{r};t), M_{\nu'}(\boldsymbol{r}';t')]\rangle_0 h_{\nu'}(\boldsymbol{r}';t').$$

The function

$$\chi_{\nu\nu'}(\boldsymbol{r},\boldsymbol{r}';t,t') \;=\; i\langle [M_\nu(\boldsymbol{r};t), M_{\nu'}(\boldsymbol{r}';t')]\rangle_0 \Theta(t-t') \tag{34}$$

is the so-called retarded response function. It is often convenient to work with the operators $\Delta M_\nu(\boldsymbol{r};t) = M_\nu(\boldsymbol{r};t) - \langle M_\nu(\boldsymbol{r})\rangle_0$ which measure the deviation with respect to the average in the absence of perturbation; since numbers always commute, we can replace $M_\nu(\boldsymbol{r};t)$ with $\Delta M_\nu(\boldsymbol{r};t)$ in the expression (34).

If the Hamiltonian H has time translational invariance symmetry the retarded response function depends only on time differences $t - t'$. For the Fourier transform we have

$$\delta\langle M_\nu(\boldsymbol{r};\omega)\rangle = \sum_{\nu'} \int d\boldsymbol{r}' \chi_{\nu\nu'}(\boldsymbol{r},\boldsymbol{r}';\omega) h_{\nu'}(\boldsymbol{r}';\omega).$$

For a lattice with lattice translational invariance, if we Fourier transform to reciprocal space and integrate over the unit cell

$$\delta\langle M_\nu(\boldsymbol{q};\omega)\rangle = \sum_{\nu'} \int d\boldsymbol{r} \int d\boldsymbol{r}' e^{i\boldsymbol{q}\cdot\boldsymbol{r}} \chi_{\nu\nu'}(\boldsymbol{q},\boldsymbol{r},\boldsymbol{r}';\omega) h_{\nu'}(\boldsymbol{q},\boldsymbol{r}';\omega).$$

Finally, if the perturbation depends on $\boldsymbol{r}'$ only through a phase we obtain

$$\delta\langle M_\nu(\boldsymbol{q};\omega)\rangle = \sum_{\nu'} \int d\boldsymbol{r} \int d\boldsymbol{r}' e^{i\boldsymbol{q}\cdot(\boldsymbol{r}-\boldsymbol{r}')} \chi_{\nu\nu'}(\boldsymbol{q},\boldsymbol{r},\boldsymbol{r}';\omega) h_{\nu'}(\boldsymbol{q};\omega) = \sum_{\nu'} \chi_{\nu\nu'}(\boldsymbol{q};\omega) h_{\nu'}(\boldsymbol{q};\omega).$$

In the $\omega = 0$ and $\boldsymbol{q} \to \boldsymbol{0}$ limit we have

$$\chi_{\nu\nu'}(\boldsymbol{0};0) = \lim_{h_{\nu'}\to 0} \frac{\partial M_\nu}{\partial h_{\nu'}},$$

where $h_{\nu'} = h_{\nu'}(\boldsymbol{0};0)$.

A.2.2 Kramers-Kronig relations and thermodynamic sum rule

Important properties of the spin susceptibility are the Kramers-Kronig relations

$$\begin{aligned} \mathrm{Re}[\chi(\boldsymbol{q};\omega)] - \mathrm{Re}[\chi(\boldsymbol{q};\infty)] &= \frac{1}{\pi}\mathcal{P}\int_{-\infty}^{+\infty} \frac{\mathrm{Im}[\chi(\boldsymbol{q};\omega')]}{\omega'-\omega} d\omega', \\ \mathrm{Im}[\chi(\boldsymbol{q};\omega)] &= -\frac{1}{\pi}\mathcal{P}\int_{-\infty}^{+\infty} \frac{\mathrm{Re}[\chi(\boldsymbol{q};\omega')] - \mathrm{Re}[\chi(\boldsymbol{q};\infty)]}{\omega'-\omega} d\omega', \end{aligned}$$

where $\mathcal{P}$ is the Cauchy principal value, and Re and Im indicate the real and imaginary part. The first Kramers-Kronig relation yields the sum rule

$$\mathrm{Re}[\chi(\boldsymbol{q};\omega=0)] - \mathrm{Re}[\chi(\boldsymbol{q};\infty)] = \frac{1}{\pi}\mathcal{P}\int_{-\infty}^{+\infty} \frac{\mathrm{Im}[\chi(\boldsymbol{q};\omega')]}{\omega'} d\omega'. \tag{35}$$

In the $\boldsymbol{q} = \boldsymbol{0}$ limit, Eq. (35) is known as *thermodynamic sum rule*.

A.2.3 Fluctuation-dissipation theorem and static susceptibility

We define the spin correlation function

$$\begin{aligned} \mathcal{S}_{\nu\nu'}(\boldsymbol{q};t) &= \langle\, \Delta S_\nu(\boldsymbol{q};t) \Delta S_{\nu'}(-\boldsymbol{q}) \rangle_0 \\ &= \langle\, S_\nu(\boldsymbol{q};t) S_{\nu'}(-\boldsymbol{q}) \,\rangle_0 - \langle S_\nu(\boldsymbol{q})\rangle_0 \langle S_{\nu'}(-\boldsymbol{q})\rangle_0 \end{aligned}$$

where $\Delta S_\nu(\boldsymbol{q};t) = S_\nu(\boldsymbol{q};t) - \langle S_\nu(\boldsymbol{q})\rangle_0$ and $\langle S_\nu(\boldsymbol{q})\rangle_0 = \langle S_\nu(\boldsymbol{q};0)\rangle_0$. The fluctuation-dissipation theorem relates $\mathcal{S}_{\nu\nu'}(\boldsymbol{q};t)$ with the magnetic susceptibility. First, one can show that the following relation holds

$$\mathrm{Im}[\chi_{\nu\nu'}(\boldsymbol{q};t)] = (g\mu_B)^2 \frac{1}{2}[\mathcal{S}_{\nu\nu'}(\boldsymbol{q};t) - \mathcal{S}_{\nu'\nu}(\boldsymbol{q};-t)]. \tag{36}$$

The correlation function has the property

$$\mathcal{S}_{\nu\nu'}(\boldsymbol{q};\omega) = e^{\beta\omega}\mathcal{S}_{\nu'\nu}(\boldsymbol{q};-\omega).$$

Thus, in ω space Eq. (36) is replaced by

$$\mathrm{Im}[\chi_{\nu\nu'}(\boldsymbol{q};\omega)] = \frac{1}{2(1+n_B)}(g\mu_B)^2\mathcal{S}_{\nu\nu'}(\boldsymbol{q};\omega), \quad n_B(\omega) = \frac{1}{e^{\beta\omega}-1}.$$

Assuming k_BT large and using Eq. (35) one can then show that

$$\mathrm{Re}[\chi_{\nu\nu'}(\boldsymbol{q};\omega=0)] - \mathrm{Re}[\chi_{\nu\nu'}(\boldsymbol{q};\infty)] \sim \frac{(g\mu_B)^2}{k_BT}\mathcal{S}_{\nu\nu'}(\boldsymbol{q};t=0).$$

A.2.4 Imaginary time and frequency response function

We define the susceptibility in imaginary time as

$$\begin{aligned}\chi_{\nu\nu'}(\boldsymbol{q};\tau,\tau') &= \langle \mathcal{T}\Delta M_\nu(\boldsymbol{q};\tau)\Delta M_{\nu'}(-\boldsymbol{q};\tau')\rangle_0 \\ &= \langle \mathcal{T}M_\nu(\boldsymbol{q};\tau)M_{\nu'}(-\boldsymbol{q};\tau')\rangle_0 - \langle M_\nu(\boldsymbol{q})\rangle_0\langle M_{\nu'}(-\boldsymbol{q})\rangle_0,\end{aligned}$$

where $\Delta M_\nu(\boldsymbol{q};\tau) = M_\nu(\boldsymbol{q};\tau) - \langle M_\nu(\boldsymbol{q};\tau)\rangle_0 = M_\nu(\boldsymbol{q};\tau) - \langle M_\nu(\boldsymbol{q})\rangle_0$. As in the case of the Green function, by using the invariance properties of the trace one can show that

$$\chi_{\nu\nu'}(\boldsymbol{q};\tau,\tau') = \chi_{\nu\nu'}(\boldsymbol{q};\tau-\tau').$$

The response function in imaginary time is related to the response function at the Bosonic Matsubara frequency $i\omega_n$ through the Fourier transforms

$$\chi_{\nu\nu'}(\boldsymbol{q};\tau) = \frac{1}{\beta}\sum_n e^{-i\omega_m\tau}\chi_{\nu\nu'}(\boldsymbol{q};i\omega_m),$$

$$\chi_{\nu\nu'}(\boldsymbol{q};i\omega_m) = \int d\tau e^{i\omega_m\tau}\chi_{\nu\nu'}(\boldsymbol{q};\tau).$$

In the rest of the Appendix we replace for simplicity the notation $\langle\rangle_0$ with $\langle\rangle$.

A.3 Magnetic susceptibility

A.3.1 Spin and magnetization operators

The spin operators S_ν are defined as

$$S_\nu = \frac{1}{2}\sum_{\sigma\sigma'} c^\dagger_\sigma \sigma_\nu c_{\sigma'},$$

where $\nu = x, y, z$ and σ_ν are the Pauli matrices

$$\sigma_x = \begin{pmatrix} 0 & 1 \\ 1 & 0 \end{pmatrix} \quad \sigma_y = \begin{pmatrix} 0 & -i \\ i & 0 \end{pmatrix} \quad \sigma_z = \begin{pmatrix} 1 & 0 \\ 0 & -1 \end{pmatrix}.$$

The magnetization operators M_ν are defined as $M_\nu = -g\mu_B S_\nu$.

A.3.2 Matsubara magnetic susceptibility

The magnetic susceptibility for a single-band system can be expressed as

$$\chi_{zz}(\boldsymbol{q};\boldsymbol{\tau}) = (g\mu_B)^2 \frac{1}{4}\sum_{\sigma\sigma'} \sigma\sigma'\, \chi^{\boldsymbol{q}\sigma\sigma'}(\boldsymbol{\tau}), \tag{37}$$

where $\sigma = 1$ or -1 depending if the spin is up or down, $\boldsymbol{\tau} = (\tau_1, \tau_2\, \tau_3, \tau_4)$ and

$$\begin{aligned} \chi^{\boldsymbol{q}\sigma\sigma'}(\boldsymbol{\tau}) &= \frac{1}{\beta}\frac{1}{N_{\boldsymbol{k}}}\sum_{\boldsymbol{k}} \chi^{\boldsymbol{q}\sigma\sigma'}_{\boldsymbol{k}}(\boldsymbol{\tau}), \\ \chi^{\boldsymbol{q}\sigma\sigma'}_{\boldsymbol{k}}(\boldsymbol{\tau}) &= \langle \mathcal{T} c_{\boldsymbol{k}\sigma}(\tau_1) c^\dagger_{\boldsymbol{k}+\boldsymbol{q}\sigma}(\tau_2) c_{\boldsymbol{k}+\boldsymbol{q}\sigma'}(\tau_3) c^\dagger_{\boldsymbol{k}\sigma'}(\tau_4)\rangle \\ &- \langle \mathcal{T} c_{\boldsymbol{k}\sigma}(\tau_1) c^\dagger_{\boldsymbol{k}+\boldsymbol{q}\sigma}(\tau_2)\rangle \langle \mathcal{T} c_{\boldsymbol{k}+\boldsymbol{q}\sigma'}(\tau_3) c^\dagger_{\boldsymbol{k}\sigma'}(\tau_4)\rangle. \end{aligned}$$

In Fourier space

$$\chi_{zz}(\boldsymbol{q}; i\omega_m) = \frac{1}{4}\sum_{\sigma\sigma'} \sigma\sigma' \frac{1}{\beta^2}\sum_{nn'} \chi^{\boldsymbol{q}\sigma\sigma'}_{n,n'}(i\omega_m),$$

where $\omega_m = 2m\pi/\beta$ is a Bosonic Matsubara frequency and

$$\chi^{\boldsymbol{q}\sigma\sigma'}_{n,n'}(i\omega_m) = \chi^{\boldsymbol{q}\sigma\sigma'}(\boldsymbol{\nu}) = \frac{1}{16}\iiiint d\boldsymbol{\tau}\; e^{i\boldsymbol{\nu}\cdot\boldsymbol{\tau}} \chi^{\boldsymbol{q}\sigma\sigma'}(\boldsymbol{\tau}).$$

The integral for each $\boldsymbol{\tau}$ component is from $-\beta$ to β and $\boldsymbol{\nu} = (\nu_n, -\nu_n - \omega_m, \nu_{n'} + \omega_m, -\nu_{n'})$.

A.3.3 Generalized Matsubara two-particle Green function

We define the generalized two-particle Green function

$$\chi^{\alpha\beta}_{\gamma\delta}(\boldsymbol{\tau}) = \langle \mathcal{T} c_\alpha(\tau_1) c^\dagger_\beta(\tau_2) c_\gamma(\tau_3) c^\dagger_\delta(\tau_4)\rangle - \langle \mathcal{T} c_\alpha(\tau_1) c^\dagger_\beta(\tau_2)\rangle \langle \mathcal{T} c_\gamma(\tau_3) c^\dagger_\delta(\tau_4)\rangle. \tag{38}$$

The Fourier transform of (38) is

$$\chi^{\alpha\beta}_{\gamma\delta}(\boldsymbol{\nu}) = \chi^{\alpha\beta\gamma\delta}_{n,n'}(i\omega_m) = \frac{1}{16}\iiiint d\boldsymbol{\tau}\; e^{i\boldsymbol{\nu}\cdot\boldsymbol{\tau}} \chi^{\alpha\beta}_{\gamma\delta}(\boldsymbol{\tau}).$$

From the symmetry properties of the trace we find that $\nu_4 = -\nu_1 - \nu_2 - \nu_3$. If we redefine $\nu_1 = \nu_n$, $\nu_2 = -\nu_n - \omega_m$, $\nu_3 = \nu_{n'} + \omega_m$, and $\nu_4 = -\nu_{n'}$ we obtain

$$\boldsymbol{\nu} = (\nu_n, -\nu_n - \omega_m, \nu_{n'} + \omega_m, -\nu_{n'}),$$

$$\chi^{\alpha\beta\gamma\delta}_{n,n'}(i\omega_m) = \frac{1}{16}\iiint d\boldsymbol{\tau}\; e^{i[-\omega_m\tau_{23}+\nu_n\tau_{12}+\nu_{n'}\tau_{34}]}\;\chi^{\alpha\beta}_{\gamma\delta}(\boldsymbol{\tau}), \tag{39}$$

where $\tau_{ij} = \tau_i - \tau_j$. The complex conjugate is given by

$$\left[\chi^{\alpha\beta\gamma\delta}_{n,n'}(i\omega_m)\right]^* = \chi^{\alpha\beta\gamma\delta}_{-n-1,-n'-1}(-i\omega_m),$$

where $\nu_{-n-1} = -\nu_n$, and $\nu_{-n'-1} = -\nu_{n'}$.

A.3.4 Symmetry properties

Let us now analyze the symmetry properties of (39). By using the fact that the response function (38) is real in τ space and by exchanging the indices 1 and 4, 2 and 3 in the integrand, we find

$$\chi^{\alpha\beta\gamma\delta}_{n,n'}(i\omega_m) = \chi^{\delta\gamma\beta\alpha}_{n',n}(i\omega_m),$$

and hence, if $\alpha = \delta$, $\beta = \gamma$, $\nu_n = \nu'_n$ is a reflection axis for the absolute value of (39)

$$\left|\chi^{\alpha\beta\gamma\delta}_{n,n'}(i\omega_m)\right| = \left|\chi^{\delta\gamma\beta\alpha}_{n',n}(i\omega_m)\right|$$

An additional reflection axis can be found by first shifting the frequency $\nu_n = \nu_l - \omega_m$

$$\chi^{\alpha\beta\gamma\delta}_{l,n'}(i\omega_m) = \frac{1}{16}\iiint d\boldsymbol{\tau}\; e^{i(-\omega_m\tau_{13}+\nu_l\tau_{12}+\nu_{n'}\tau_{34})}\chi^{\alpha\beta}_{\gamma\delta}(\boldsymbol{\tau})$$

and then exchanging in the integrand the indices 12 with 34 and vice versa. Hence

$$\chi^{\alpha\beta\gamma\delta}_{l,n'}(i\omega_m) = \chi^{\gamma\delta\alpha\beta}_{n',l}(-i\omega_m)$$

so that, if $\alpha = \gamma$ and $\beta = \delta$, $\nu_{n+m} = -\nu_{n'}$ is a mirror line

$$\left|\chi^{\alpha\beta\gamma\delta}_{n+m,n'}(i\omega_m)\right| = \left|\chi^{\gamma\delta\alpha\beta}_{-n'-1,-n-m-1}(i\omega_m)\right|.$$

A.3.5 Non interacting limit

For a non-interacting system Wick's theorem yields

$$\begin{aligned}\chi^{\alpha\beta}_{\gamma\delta}(\boldsymbol{\tau}) &= -\langle\mathcal{T}c_\alpha(\tau_1)c^\dagger_\delta(\tau_4)\rangle\langle\mathcal{T}c_\gamma(\tau_3)c^\dagger_\beta(\tau_2)\rangle \\ &= -G_{\alpha\delta}(\tau_{14})G_{\gamma\beta}(-\tau_{23}).\end{aligned}$$

We take as example the one band model (29) and set $\alpha = \boldsymbol{k}\sigma$, $\beta = \boldsymbol{k}+\boldsymbol{q}\sigma$, $\gamma = \boldsymbol{k}+\boldsymbol{q}\sigma'$, and $\delta = \boldsymbol{k}\sigma'$. Then, in the paramagnetic case, the magnetic susceptibility is given by

$$\chi_{zz}(\boldsymbol{q};\boldsymbol{\tau}) = -(g\mu_B)^2\frac{1}{4}\frac{1}{\beta}\frac{1}{N_{\boldsymbol{k}}}\sum_{\boldsymbol{k}}\sum_{\sigma}\mathcal{G}_{\boldsymbol{k}\sigma}(\tau_{14})\mathcal{G}_{\boldsymbol{k}+\boldsymbol{q}\sigma}(\tau_{32}).$$

Its Fourier transform is

$$\chi_{zz}(\boldsymbol{q};i\omega_m) \;=\; (g\mu_B)^2\frac{1}{4}\frac{1}{\beta^2}\sum_{nn'}\sum_{\sigma}\chi^{\boldsymbol{q}\sigma\sigma}_{n,n'}(i\omega_m),$$

where

$$\sum_{\sigma}\chi^{\boldsymbol{q}\sigma\sigma}_{n,n'}(i\omega_m) = -\beta\frac{1}{N_{\boldsymbol{k}}}\sum_{\boldsymbol{k}}\sum_{\sigma}\mathcal{G}_{\boldsymbol{k}\sigma}(i\nu_n)\mathcal{G}_{\boldsymbol{k}+\boldsymbol{q}\sigma}(i\nu_n+i\omega_m)\delta_{n,n'}.$$

Thus the static susceptibility is

$$\chi_{zz}(\boldsymbol{q};0) \;=\; -\left(g\mu_B\right)^2\frac{1}{4}\frac{1}{N_{\boldsymbol{k}}}\sum_{\boldsymbol{k}}\sum_{\sigma}\frac{n_\sigma(\varepsilon_{\boldsymbol{k}+\boldsymbol{q}})-n_\sigma(\varepsilon_{\boldsymbol{k}})}{\varepsilon_{\boldsymbol{k}+\boldsymbol{q}}-\varepsilon_{\boldsymbol{k}}}.$$

Finally, in the $\boldsymbol{q}\to 0$ and $T\to 0$ limit we find

$$\begin{aligned}\chi_{zz}(\mathbf{0};0) &= \frac{1}{4}\left(g\mu_B\right)^2\rho(\varepsilon_F)\\ \rho(\varepsilon_F) &= -\sum_{\sigma}\frac{1}{N_{\boldsymbol{k}}}\sum_{\boldsymbol{k}}\left.\frac{dn_\sigma(\varepsilon_{\boldsymbol{k}})}{d\varepsilon_{\boldsymbol{k}}}\right|_{T=0}\end{aligned}$$

A.3.6 Atomic limit

We calculate the local atomic susceptibility for the system described by the Hamiltonian (31) starting from the general expression (38). In the sector $\tau_i > \tau_{i+1}$ we have

$$\chi^{\sigma\,\sigma}_{\sigma'\sigma'}(\boldsymbol{\tau}) = \frac{1}{2(1+e^{\beta U/2})}\left(e^{\tau_{12}U/2+\tau_{34}U/2}+\delta_{\sigma\sigma'}e^{(\beta-\tau_{12})U/2-\tau_{34}U/2}\right).$$

The magnetic susceptibility for $\tau_i > \tau_{i+1}$ is then given by

$$\chi_{zz}(\boldsymbol{\tau}) = \left(g\mu_B\right)^2\frac{1}{4}\frac{1}{\beta}\sum_{\sigma\sigma'}\sigma\sigma'\chi^{\sigma\,\sigma}_{\sigma'\sigma'}(\boldsymbol{\tau}) = \frac{\left(g\mu_B\right)^2}{4\beta}\frac{1}{(1+e^{\beta U/2})}e^{(\beta-\tau_{12}-\tau_{34})U/2},$$

which depends only on $\tau_{12}+\tau_{34}$. If we perform the Fourier transform we recover formula for the uniform static susceptibility

$$\chi_{zz}(\mathbf{0};0) = \left(g\mu_B\right)^2\frac{1}{4k_BT}\frac{e^{\beta U/2}}{1+e^{\beta U/2}} = \left(g\mu_B\right)^2\frac{1}{4}\frac{1}{\beta^2}\sum_{nn'}\sum_{\sigma\sigma'}\sigma\sigma'\,\chi^{\mathbf{0}\sigma\sigma'}_{n,n'}(0),$$

where

$$\sum_{\sigma\sigma'}\sigma\sigma'\,\chi^{\mathbf{0}\sigma\sigma'}_{n,n'}(i\omega_m) \;=\; \beta\frac{1}{i\nu_n-U/2}\frac{1}{i\nu_{n'}-U/2}\frac{1+e^{\beta U/2}}{e^{\beta U/2}}\delta_{\omega_m,0}.$$

A.3.7 Alternative formulation

The spin susceptibility can also be obtained from $\chi^{i,i'}_{zz}(\boldsymbol{\tau})$ with $\boldsymbol{\tau} = (\tau_1, \tau_1, \tau_3, \tau_3)$. We have

$$\chi^{i,i'}_{zz}(\boldsymbol{\tau}) = \chi^{i,i'}_{zz}(\tau_{13}) \;\; = \;\; \langle \mathcal{T} M^i_z(\tau_1) M^{i'}_z(\tau_3)\rangle - \langle M^i_z\rangle\langle M^{i'}_z\rangle,$$

where $M^i_z = -g\mu_B S^i_z$ is the magnetization at site i. Its Fourier transform is

$$\chi^{i,i'}_{zz}(i\omega_m) \;\; = \;\; \int d\tau_{13} e^{i\omega_m \tau_{13}} \chi^{i,i'}_{zz}(\tau_{13}).$$

By Fourier transforming to the reciprocal space we find

$$\begin{aligned}
\chi_{zz}(\boldsymbol{q};\tau_{13}) &= \langle \mathcal{T} M_z(\boldsymbol{q};\tau_1) M_z(-\boldsymbol{q};\tau_3)\rangle - \langle M_z(\boldsymbol{q})\rangle\langle M_z(-\boldsymbol{q})\rangle, \\
\chi_{zz}(\boldsymbol{q};i\omega_m) &= \int d\tau e^{i\omega_m \tau_{13}} \chi_{zz}(\boldsymbol{q};\tau_{13}).
\end{aligned}$$

References

[1] H. Bruus and K. Flensberg: *Many-Body Quantum Theory in Condensed Matter Physics* (Oxford University Press, 2004)

[2] P. Fazekas: *Lecture Notes on Electron Correlation and Magnetism* (World Scientific, Singapore, 1999)

[3] D.C. Matthis: *The Theory of Magnetism Made Simple* (World Scientific, Singapore, 2006)

[4] K. Yosida: *Theory of Magnetism* (Springer, Heildelberg, 1998)

[5] A.C. Hewson: *The Kondo Problem to Heavy Fermions* (Cambridge University Press, 1993)

[6] E. Pavarini, E. Koch, A. Lichtenstein, D. Vollhardt: *The LDA+DMFT approach to strongly correlated materials*, Reihe Modeling and Simulation, Vol. 1 (Forschungszentrum Jülich, 2011) `http://www.cond-mat.de/events/correl11`

[7] E. Pavarini, E. Koch, F. Anders, M. Jarrell: *Correlated electrons: from models to materials*, Reihe Modeling and Simulation, Vol. 2 (Forschungszentrum Jülich, 2012) `http://www.cond-mat.de/events/correl12`

[8] See R. Eder, *Multiplets in Transition Metal Ions* in Ref. [7]

[9] See E. Pavarini, *Crystal-field Theory, Tight-binding Method and Jahn-Teller Effect*, in Ref. [7]

[10] See E. Pavarini, *The LDA+DMFT Approach*, in Ref. [6]

[11] See E. Koch, *Exchange Mechanisms*, in Ref. [7]

[12] J.R. Schrieffer and P.A. Wolff, Phys. Rev. **149**, 491 (1966); A.H. MacDonald, S.M. Girvin and D. Yoshioka, Phys. Rev. B **37**, 9753 (1988)

[13] E. Pavarini, I. Dasgupta, T.Saha-Dasgupta, O. Jepsen and O.K. Andersen, Phys. Rev. Lett. **87**, 047003 (2001)

[14] K. Wilson, Rev. Mod. Phys. **47**, 773 (1975)

[15] N. Andrei, K. Furuya, and J.H. Lowenstein, Rev. Mod. Phys. **55**, 331 (1983); A.M. Tsvelik and P.B. Wiegmann, Adv. Phys. **32**, 453 (1983)

[16] J.E. Gubernatis, J.E. Hirsch, and D.J. Scalapino,
Phys. Rev. B **16**, 8478 (1987)

[17] P.W. Anderson, J. Phys. C: Solid State Phys. **3**, 2436 (1970)

[18] E. Pavarini and L.C. Andreani, Phys. Rev. Lett. **77**, 2762 (1996)

[19] P. Nozières, J. Low. Temp. Phys. **17**, 31 (1974)

[20] A.I. Lichtenstein, M.I. Katsnelson, and V.A. Gubanov, J. Phys. F **14**, L125;
Solid State Commun. **54**, 327 (1985);
A.I. Lichtenstein, M.I. Katsnelson, V.P. Antropov, and V.A. Gubanov,
J. Magn. Magn. Mater. **67**, 65 (1987);
M.I. Katsnelson and A.I. Lichtenstein, Phys. Rev. B **61**, 8906 (2000)

[21] E. Pavarini, E. Koch, and A.I. Lichtenstein,
Phys. Rev. Lett. **101**, 266405 (2008);
A. Chiesa, S. Carretta, P. Santini, G. Amoretti and E. Pavarini,
Phys. Rev. Lett. **110**, 157204 (2013)